



Background Document

FEMA P-58/BD-3.8.7

Fragility Curves for Slab-Column Connections

Prepared by

Aysegul Gogus and John W. Wallace
Department of Civil & Environmental Engineering
5731 Boelter Hall
University of California, Los Angeles
Los Angeles, California 90095

Submitted to

APPLIED TECHNOLOGY COUNCIL
201 Redwood Shores Parkway, Suite 240
Redwood City, California 94065
www.ATCouncil.org

Prepared for

FEDERAL EMERGENCY MANAGEMENT AGENCY
U.S. Department of Homeland Security
500 C Street, SW
Washington, D.C. 20472

November 1, 2008



FEMA



Background Documentation

FEMA P-58 Background Documents are a series of reports documenting the technical background and source information for key aspects of the FEMA P-58 methodology and its implementation. These reports were developed over the course of the 10-year ATC-58/ATC-58-1 Projects funded under FEMA Contracts EMW-2001-RP-0056 and HSFEHQ-06-D-1105.

Background Documents were developed by consultants, serving at various levels within the project hierarchy, reporting the results of: (1) decisions on technical development protocols; (2) focused studies on the development of key aspects of the methodology; (3) documentation of recommended procedures; and (4) collection of available data for the development of structural and nonstructural fragilities. They were initially intended to serve as a record of the technical state-of-knowledge at the time they were produced, and as resources for the development of the eventual project reports. As such, they represent a snapshot in time, and may, or may not, match the technical content, recommended procedures, or data incorporated into the final methodology and its implementation.

This Background Document is intended for the purpose of providing supplemental knowledge to users of the FEMA P-58 methodology. Information contained herein has not been independently verified for accuracy as a stand-alone document, and may have been superseded in its final implementation within the methodology. Users of information in this document assume all liability arising from such use.

Notice

Any opinions, findings, conclusions, or recommendations expressed in this publication do not necessarily reflect the views of the Applied Technology Council (ATC), the Department of Homeland Security (DHS), or the Federal Emergency Management Agency (FEMA). Additionally, neither ATC, DHS, FEMA, nor any of their employees, makes any warranty, expressed or implied, nor assumes any legal liability or responsibility for the accuracy, completeness, or usefulness of any information, product, or process included in this publication. Users of information from this publication assume all liability arising from such use.

Cover illustration – Primary resource documents for the FEMA P-58 *Seismic Performance Assessment of Buildings, Methodology and Implementation* series of products: FEMA P-58-1, *Volume 1 – Methodology*, and FEMA P-58-2, *Volume 2 – Implementation Guide*.

FRAGILITY CURVES FOR SLAB-COLUMN CONNECTIONS

AYSEGUL GOGUS

JOHN W. WALLACE

UNIVERSITY OF CALIFORNIA, LOS ANGELES
DEPARTMENT OF CIVIL & ENVIRONMENTAL ENGINEERING

Final Report to the
Applied Technology Council: Project ATC-58

November 2008

ABSTRACT

Development of fragility curves is important for performance based earthquake engineering to define damage states as a function of engineering demand parameter (EDP), such as inter-story drift. As part of an effort to develop fragility curves for new slab-column frame construction, existing test data from seventy one tests were collected and reviewed. Based on this review, backbone curves for each specimen were formed and damage states were defined. Fragility curves for yielding of flexural reinforcement and punching failure, corresponding to different gravity shear ratio (V_g/V_0) ranges, are developed for the following connection types: (1) reinforced concrete slab-column connections without shear reinforcement, (2) reinforced concrete slab-column connections with shear reinforcement, and (3) post-tensioned slab-column connections without shear reinforcement. The degree of slab-column connection damage reported for these states (yielding and punching) is reviewed to derive fragility relations for two repair states, minor repair associated with epoxy injection of cracks to restore stiffness and major repair to restore stiffness and strength. Test results reported in the literature also were used to estimate crack lengths requiring epoxy injection for each type of connection. Given the lack of test data for post-tensioned slab-column connections with shear reinforcement and reinforced concrete slab-column connections with shear capitals or drop panels, fragility curves for the two repair states for these connection types were derived based on engineering judgment.

TABLE OF CONTENTS

ABSTRACT	iii
TABLE OF CONTENTS	iv
LIST OF FIGURES	v
LIST OF TABLES	vii
1. INTRODUCTION	1
2. ORGANIZATION	6
3. SOURCES OF INFORMATION.....	7
3.1. REINFORCED CONCRETE SPECIMENS WITHOUT SHEAR REINFORCEMENT	7
3.2. REINFORCED CONCRETE SPECIMENS WITH SHEAR REINFORCEMENT	8
3.3. POST-TENSIONED SPECIMENS WITHOUT SHEAR REINFORCEMENT	8
4. DAMAGE STATES.....	8
5. FRAGILITY CURVES	11
5.1. METHODOLOGY	11
5.2. DAMAGE AND REPAIR STATES	13
6. CRACK PATTERNS AND IMAGES	26
REFERENCES.....	31
APPENDICES	34

LIST OF FIGURES

Figure 1.1	Definition of Slab Critical Section	2
Figure 1.2	Drift Ratio at Punching versus Gravity Shear Ratio, ASCE 41-06.....	5
Figure 4.1	Illustrative Backbone Curve and Idealized Elasto-Plastic Relation	10
Figure 5.1	Punching Failure for RC Connections without Shear Reinforcement with Significant Drop in Floor Slab by Hwang and Moehle, 1989 – Major Repair Required	17
Figure 5.2	Punching Failure for PT Connection without Shear Reinforcement with Significant Drop in Floor Slab by Kang, 2006 – Major Repair Required	17
Figure 5.3	Fragility Curves for RC Connections without Shear Reinforcement, $0 \leq \text{GSR} < 0.2$	20
Figure 5.4	Fragility Curves for RC Connections without Shear Reinforcement, $0.2 \leq \text{GSR} < 0.4$	20
Figure 5.5	Fragility Curves for RC Connections without Shear Reinforcement, $0.4 \leq \text{GSR} < 0.6$	21
Figure 5.6	Fragility Curves for RC Connections with Shear Reinforcement, $0 \leq \text{GSR} < 0.2$ & $0.2 \leq \text{GSR} < 0.4$	21
Figure 5.7	Fragility Curves for RC Connections with Shear Reinforcement, $0.4 \leq \text{GSR} < 0.6$	22
Figure 5.8	Fragility Curves for PT Connections without Shear Reinforcement, $0 \leq \text{GSR} < 0.2$ & $0.2 \leq \text{GSR} < 0.4$	22
Figure 5.9	Fragility Curves for PT Connections without Shear Reinforcement, $0.4 \leq \text{GSR} < 0.6$	23
Figure 5.10	Fragility Curves for Shear Reinforced PT Connections, $0 \leq \text{GSR} < 0.2$ & $0.2 \leq \text{GSR} < 0.4$	23
Figure 5.11	Fragility Curves for Shear Reinforced PT Connections, $0.4 \leq \text{GSR} < 0.6$	24

Figure 5.12	Fragility Curves for RC Connections with Shear Capitals/Drop Panels, $0 \leq \text{GSR} < 0.2$ & $0.2 \leq \text{GSR} < 0.4$	24
Figure 5.13	Fragility Curves for RC Connections with Shear Capitals/Drop Panels, $0.4 \leq \text{GSR} < 0.6$	25
Figure B1	Illustrative Uniaxial Cyclic Loading History of an Interior Specimen by Stark, Binici and Bayrak, 2005	41
Figure B2	Illustrative Repeated Loading Configuration of an Exterior Specimen by Trongtham and Hawkins, 1977	42
Figure B3	Illustrative Repeated Loading History by Dilger and Shatila, 1989	42
Figure C1	Illustrative Test Configuration of an Interior Specimen by Robertson and Johnson, 2006	42
Figure C2	Illustrative Test Configuration of an Exterior Specimen by Martinez- Cruzado, 1993	43
Figure D1	Hysteretic Response and Backbone Curve for Specimen 2CS by Robertson, Kawai, Lee, and Enomoto, 2002	43

LIST OF TABLES

Table 5.1	Collected Data for Yielding and Punching States for Reinforced Concrete Specimens without Shear Reinforcement.....	12
Table 5.2	Specimen Size Parameters of the Bins.....	15
Table 5.3	Damage States and the Associated Parameters.....	16
Table 5.4	Parameters of the Fragility Functions for Connection Types 1, 2 and 3	18
Table 5.5	Parameters of the Fragility Functions for Connection Types 4 and 5	19
Table 6.1	Crack Patterns of DS1.....	27
Table 6.2	Crack Patterns and Images of DS2	29
Table A1	Parameters of the Reinforced Concrete Specimens without Shear Reinforcement, $0 \leq \text{GSR} < 0.2$	34
Table A2	Parameters of the Reinforced Concrete Specimens without Shear Reinforcement, $0.2 \leq \text{GSR} < 0.4$	35
Table A3	Parameters of the Reinforced Concrete Specimens without Shear Reinforcement, $0.4 \leq \text{GSR} < 0.6$	36
Table A4	Parameters of the Reinforced Concrete Specimens with Shear Reinforcement, $0.2 \leq \text{GSR} < 0.4$	36
Table A5	Parameters of the Reinforced Concrete Specimens with Shear Reinforcement, $0.4 \leq \text{GSR} < 0.6$	37
Table A6	Parameters of the Post-Tensioned Specimens without Shear Reinforcement, $0.2 \leq \text{GSR} < 0.4$	38
Table A7	Parameters of the Post-Tensioned Specimens without Shear Reinforcement, $0.4 \leq \text{GSR} < 0.6$	39
Table B1	Illustrative Uniaxial Cyclic Load History of an Interior Specimen by Stark, Binici and Bayrak, 2005	41

Table E1	Collected Data for Yielding and Punching States of Reinforced Concrete Specimens without Shear Reinforcement.....	44
Table E2	Collected Data for Yielding and Punching States of Post-Tensioned Reinforced Concrete Specimens without Shear Reinforcement	45

1. Introduction

This document summarizes the development of fragility curves for slab-column connections. Two general types of connections are considered, reinforced concrete and post-tensioned reinforced concrete, both with and without slab shear reinforcement. Failure of slab-column connections are typically associated with punching failures, either prior to or after flexural yielding of the slab flexural reinforcement. Punching failures are typically abrupt and result in substantial strength loss. Complete collapse of slab-column systems, often referred to as “pancake-type” failure, can occur if sufficient continuous slab bottom reinforcement is not provided. Per ACI 318 requirements for integrity reinforcement, at least two continuous bottom reinforcement bars must be anchored within the column.

Prior research (e.g., Moehle, 1996; FEMA 356) has shown that the punching failures are highly dependent on the magnitude of the applied slab gravity shear stress at the slab-column critical section and the magnitude of the lateral displacement applied to the connection. Given these findings, for this study, story drift was established as the Demand Parameter (DP) and specific connection types were binned according to the Gravity Shear Ratio (GSR) for the slab-column critical section for the various types of connection types considered. Story drift is defined as the relative displacement in a given story divided by the story height, or in the case of slab-connections, it is often defined as the average of the story drift values for the story above and below the level of the slab-column connection of interest. Gravity Shear Ratio (GSR) is defined to be the ratio of the factored gravity shear force acting on the slab critical section ($V_u = V_g$) divided by the nominal concrete shear strength of the slab critical section defined by ACI 318-08 Chapter 11 for connections without slab shear reinforcement (i.e., $V_n = V_c$): i.e., $GSR = V_u / \phi V_n = V_g / \phi V_c$.

According to ACI 318-08 §11.11.2.1, the nominal concrete capacity of slab-column critical section for non-prestressed connections is taken as the minimum of:

$$(a) V_c = \left(2 + \frac{4}{\beta}\right) \sqrt{f'_c} b_0 d \quad \text{ACI 318-08 Equation (11-31)}$$

$$(b) V_c = \left(\frac{\alpha d}{b_0} + 2\right) \sqrt{f'_c} b_0 d \quad \text{ACI 318-08 Equation (11-32)}$$

$$(c) V_c = 4 \sqrt{f'_c} b_0 d \quad \text{ACI 318-08 Equation (11-33)}$$

where, f'_c is the compressive strength of concrete, d is the distance from extreme compression fiber to centroid of the longitudinal tension reinforcement (average value if two layers), β is the ratio of long to short dimensions (for clear slab spans, sides of columns, or concentrated load or reaction area), α_s is 40 for interior columns, 30 for exterior columns and 20 for corner columns, and b_0 is the perimeter of the critical section of the slab at a distance of $d/2$ away from the face of the column (Figure 1.1).

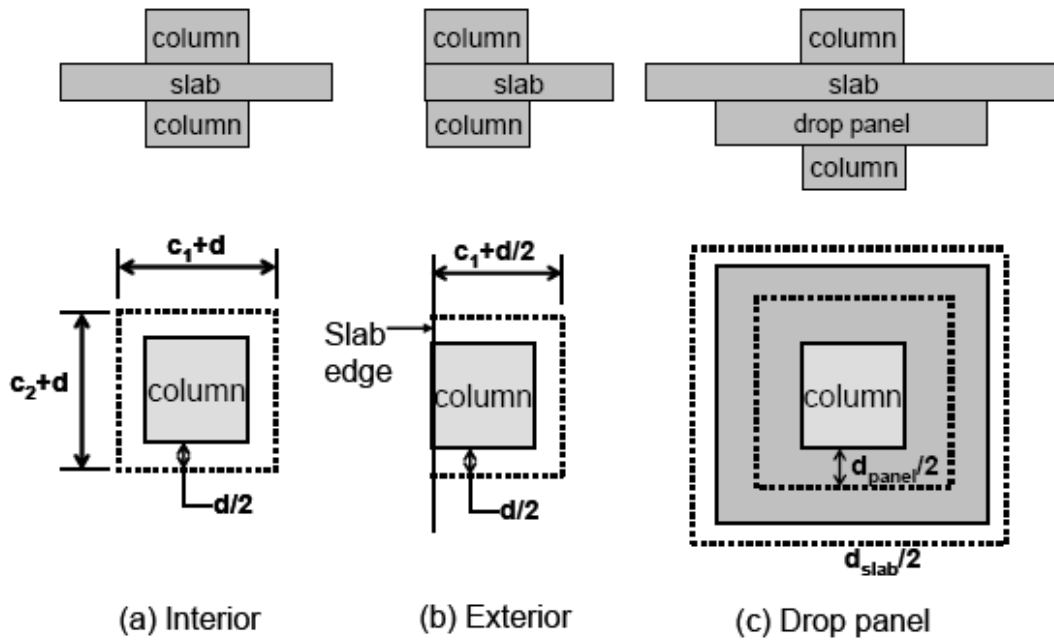


Figure 1.1: Definition of slab critical section (see ACI 318-08 §11.11.1.2)

For prestressed slabs, ACI 318-08 §11.11.2.2 defines V_c as:

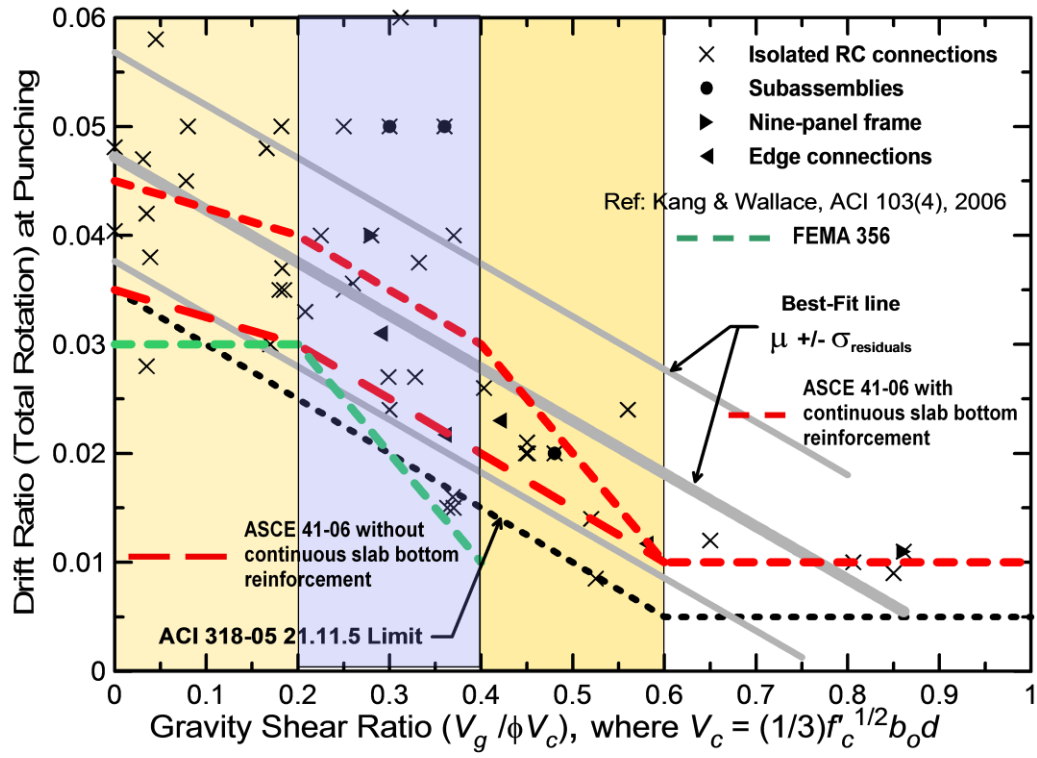
$$V_c = (\beta_p \sqrt{f'_c} + 0.3 f_{pc}) b_0 d + V_p \quad \text{ACI 318-05 Equation (11-34)}$$

where β_p is the smaller of 3.5 and $(\alpha_s d/b_0 + 1.5)$, f_{pc} is the average value of the compressive stress for the two directions, V_p is the vertical component of all effective pre-stress forces crossing the critical section, and α_s and b_0 are as pre-mentioned. Equation (11-34) is valid only if the following conditions are satisfied: (a) no portion of the column cross-section shall be closer to a discontinuous edge than 4 times the slab thickness; (b) the value of $\sqrt{f_c'}$ used in the ACI 318-08 equation (11-34) shall not be taken greater than 70 psi; and (c) in each direction, f_{pc} shall not be less than 125 psi, nor be taken greater than 500 psi. Otherwise, V_c is computed using the procedure given in ACI 318-08 11.11.2.1, described above by Equations (11-31), (11-32), and (11-33).

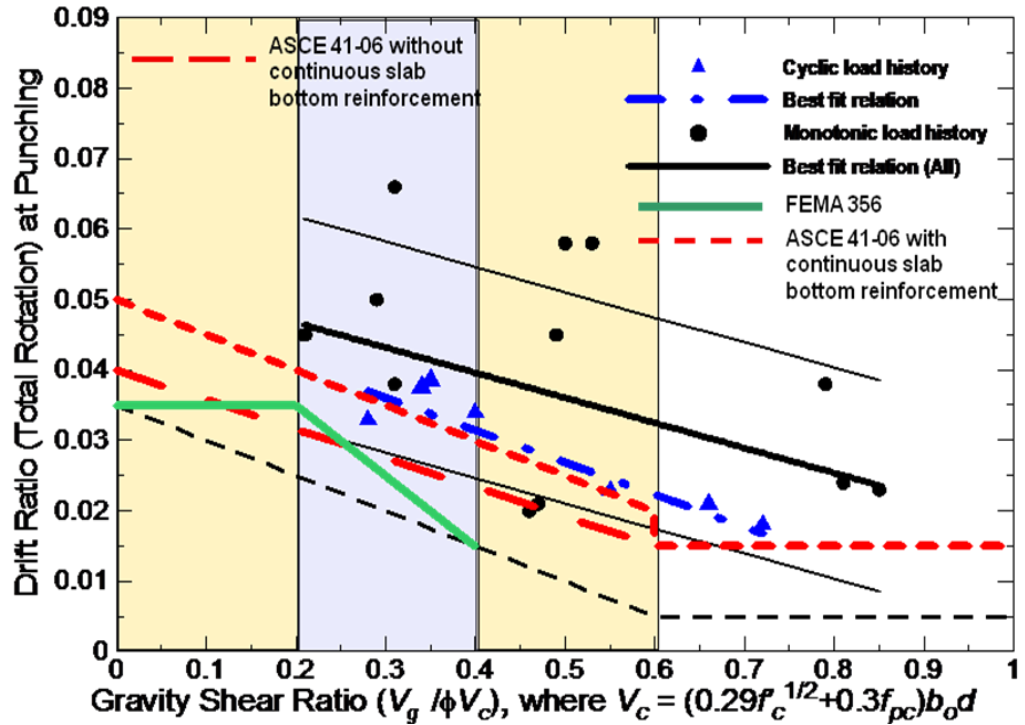
The relationships between story drift and GSR for three types of connections, RC connections with and without shear reinforcement and PT connections without shear reinforcement, are given in Figure 1.2 (Kang and Wallace, 2006). The FEMA 356 Pre-Standard Table 6-14 lists allowable plastic rotations for GSR ranges of: (a) $\text{GSR} < 0.2$; (b) $0.2 \leq \text{GSR} \leq 0.4$; and (c) $0.4 < \text{GSR}$ to capture the trends noted in Figure 1.2 for reinforced concrete connections with and without continuous slab bottom reinforcement. A similar approach was taken in ASCE 41-06, including Supplement #1 (Table 6-14); however, results were provided for both reinforced concrete and post-tensioned connections, and results were placed into more bins to more accurately reflect the trends noted in Figure 1.2. Allowable plastic rotation values given in ASCE 41-06 (Figure 1.2), including Supplement #1, approximately reflect the mean minus one standard deviation values for connections with and without continuity reinforcement, respectively (Elwood et al., 2007). The ATC-58 performance-based seismic design framework requires development of fragility relations, versus the deterministic approach employed in these prior documents (FEMA 356, ASCE 41-06). Consistent with ASCE 41-06 and Figure 1.2(a), the fragility relations developed apply to both interior and exterior (edge) connections. The derived fragility relations apply to slab-column connections with continuous bottom reinforcement since, with the exception of three specimens with post-tensioning, all test specimens have continuous bottom reinforcement either parallel and/or perpendicular to the direction of the applied loading. Therefore, insufficient data exist to derive fragility curves for specimens without continuous bottom reinforcement. To address this gap, we recommend using the relations derived for slabs with continuous bottom

reinforcement; however, limiting the probability of major repair (punching failure) to a low value (e.g., 5 or 10%) because punching failure for slab-column connections without continuous slab bottom reinforcement (or post-tensioning) is very likely to lead to collapse.

It should be noted that the fragility relations derived for the two repair states (epoxy repair and major repair, defined in Table 5.3) were generally based on observations from only eight to nine specimens per bin. It is noted that specimen sizes (scale), material properties, slab span to depth ratios, reinforcement (grade, quantities, distributions, see Appendix A), and loading conditions (see Appendix B) vary and would be expected to impact the demand parameters (especially given the relatively small number of available tests). Additional data within each bin would be helpful to derive more reliable fragility functions and to develop better estimates of crack patterns for the damage states. However, it is noted that the variation in the test results across the bins is similar, and thus, the test data are sufficient to accomplish the desired objectives. An alternative format to that presented would be to develop fragility functions that are continuous with GSR. This approach was considered, but not adopted, such that the results of this study are consistent with prior results (e.g., FEMA 356, ASCE 41).



(a) Reinforced concrete specimens without shear reinforcement



(b) Post-tensioned specimens without shear reinforcement

Figure 1.2: Drift ratio at punching versus gravity shear ratio, ASCE 41-06,
(V_c in metric units)

2. Organization

Material was presented in the prior section to provide the background information necessary to support the development of fragility relations for slab-column connections. Fragility relations are developed for a variety of connection types for specific ranges of GSR. The connection types considered include:

- (1) Reinforced concrete slab-column connections without shear reinforcement
- (2) Reinforced concrete slab-column connections with shear reinforcement
- (3) Post-tensioned slab-column connections without shear reinforcement
- (4) Post-tensioned slab-column connections with shear reinforcement
- (5) Reinforced concrete slab-column connections with shear capitals and/or drop panels

Based on available data, and to be consistent with existing documents (e.g., ASCE 41-06), two GSR ranges were considered for each connection type:

- (i) $0.2 \leq V_g/V_0 < 0.4$
- (ii) $0.4 \leq V_g/V_0 < 0.6$

Sufficient data were available for reinforced concrete connections without shear reinforcement to include a third GSR range between $0 \leq V_g/V_0 < 0.2$. For the remaining connection types, use of the fragility relations developed for GSR between $0.2 \leq V_g/V_0 < 0.4$ provide a conservative estimate of damage for GSR less than 0.2.

An upper limit of $GSR = 0.6$ was selected because very limited data exist for connections tested at higher GSR values, and because a GSR greater than 0.6 is not practical (otherwise punching failure would occur at a very low drift ratio). As previously noted, bins for GSR between 0.2 to 0.4 and 0.4 to 0.6 were selected to be consistent with prior work (e.g., FEMA 356, ASCE 41-06).

The fragility curves for connection types (1), (2) and (3) are developed using data from laboratory tests. Based on the observed behavior of slab-column connections under lateral loadings, fragility relations for two ordered damage states are defined (yielding and punching) and used to derive two ordered repair states (epoxy injection and major repair). Insufficient data exists to develop fragility relations for connection types (4) and (5); therefore, relations for these

cases were derived using results obtained for connection types (1), (2) and (3) based on judgment.

3. Sources of Information

Data sources and the specimen details (geometry, reinforcement, material properties) are tabulated in Appendix A. Illustrative loading protocols are given in Appendix B, and the test frame configurations are given in Appendix C. Test data for specimens constructed with lightweight or high strength concrete, or for monotonic loading, are not included in the database as there are relatively few tests for these cases and the limited data available. The limited data indicate that these specimens are generally capable of reaching larger story drift ratios prior to reaching a prescribed damage state compared with tests for normal strength and normal weight concrete, and for monotonic loading (Kang and Wallace, 2006). Therefore, the results reported apply only to connections constructed with normal weight and normal strength concrete, but may be used as estimates for lightweight or high strength concrete, and monotonic loading. Test data for specimens with slab openings also were not included in the database, as there are relatively few tests and these specimens. In general, specimens with openings would be expected to achieve lower story drift ratios prior to reaching a prescribed damage state, compared with tests without openings. A summary of the test data used to assess the performance and damage states is provided below.

3.1. Reinforced concrete specimens without shear reinforcement

i. $0 < V_g/V_0 < 0.2$

Data from a total of seven laboratory tests from four different investigations were reviewed; all specimens were cyclically loaded (cyclic loading \equiv reversed cyclic loading).

ii. $0.2 \leq V_g/V_0 < 0.4$

Data from a total of seventeen laboratory tests from ten different investigations were reviewed; all specimens were cyclically loaded.

iii. $0.4 \leq V_g/V_0 \leq 0.6$

Data from a total of nine laboratory tests from six different investigations were reviewed; all specimens were cyclically loaded.

3.2. Reinforced concrete specimens with shear reinforcement

i. $0.2 < V_g/V_0 < 0.4$

Data from a total of ten laboratory tests from four different investigations were reviewed. Shear reinforcement consisted of: four specimens with closed hoop stirrups, four specimens with thin plate stirrups, one specimen with single leg stirrups, and two specimens with headed studs. All of the specimens were cyclically loaded.

ii. $0.4 \leq V_g/V_0 \leq 0.6$

Data from a total of twelve laboratory tests from three different investigations were reviewed. Shear reinforcement consisted of: two specimens with carbon fiber-reinforced polymer “stirrups”, nine specimens with headed studs, and one specimen with headed stirrups. All of the specimens were cyclically loaded.

3.3. Post-tensioned specimens without shear reinforcement

i. $0.2 < V_g/V_0 < 0.4$

Data from a total of nine laboratory tests from five different investigations were reviewed. One test specimen was subjected to repeated loading, while the remaining nine specimens were cyclically loaded. Illustration of repetitive loading is provided in Appendix B (ii).

ii. $0.4 \leq V_g/V_0 \leq 0.6$

Data from a total of seven laboratory tests from six different investigations were reviewed. Two of the test specimens were subjected to repeated loading, while the remaining five specimens were cyclically loaded.

4. Damage States

The primary goal of the project is to define two repair states, one associated with modest repair requiring epoxy injection of cracks, and the other associated with major repair (e.g., shoring, removing damaged concrete, possibly jacking, and placing new concrete). However, these damage states are rarely noted in the literature for any given test, and thus, had to be inferred from available data. Significant residual crack widths following an earthquake exist only when strains in slab flexural reinforcement exceed the yield strain, whereas major repair is more likely to be associated with punching failures. Therefore, to guide the process of fragility curve development for the two prescribed repair states, fragility relations for two well-defined damage states were initially determined, and then used to derive the fragility relations associated with the repair states. The two damage states are: (a) yielding of the specimen and (b) immediate/gradual drop in the lateral load capacity, referred to as punching failure. The procedure used to obtain the fragility relations for these two damage states is described in the following paragraphs.

A generalized lateral load versus lateral displacement relation, or a backbone curve, for a representative test of an isolated slab-column connection is given in Figure 4.1. Backbone curves are obtained using the ASCE 41-06 Supplement #1 procedure, i.e., by connecting the peak points on the load versus displacement relation for the first cycle at each prescribed load or displacement level (see Appendix D, Figure D1). Important damage states identified on the backbone curves were selected to be yielding and punching. Due to the nonlinearity of the backbone curve near the yield point, an idealized elastoplastic relation was defined as suggested by Pan and Moehle (1989) using an horizontal line to provide an estimate of the peak lateral load, and an initial slope based on a secant defined at two-thirds of the peak load (Figure 4.1).

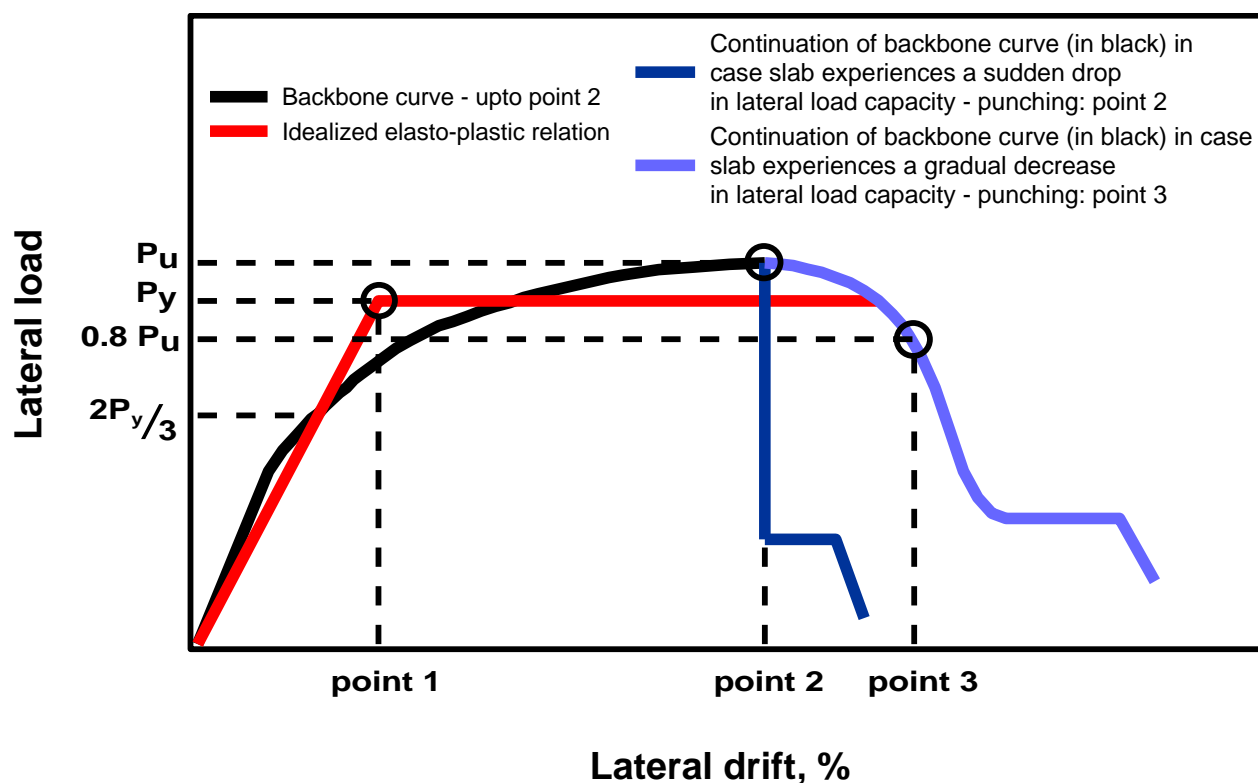


Figure 4.1: Illustrative backbone curve and idealized elasto-plastic relation

Damage states, defined on Figure 4.1, correspond to the following points:

Point 1 – Yield: The point that corresponds to the intersection of the elastic and the plastic portion of the idealized elasto-plastic relation, referred to as the yield point.

Point 2 - Peak lateral load: The point corresponding to the peak lateral load. In case the lateral load carrying capacity of the slab drops suddenly after the peak point (shown in dark blue in Figure 4.1), point 2 is referred to as the punching (failure) point.

Point 3 - Strength loss: The point on the load versus displacement relation corresponding to 20% drop from the peak load; which is consistent with commonly used values (15 to 20%) to define significant strength loss (e.g., ASCE 41-06 S3.4.3). In general, this point is defined by one of three conditions: (a) A very distinct and significant drop in lateral load (punching failure) occurs at the peak lateral load and point 3 is the same as point 2, (b) punching failure occurs at a lateral displacement that exceeds the value of point 2 and the lateral load at punching failure is less than the peak load, but greater than 80% of the peak load, and (c) the drop in lateral load is more gradual, and punching failure is defined by a 20% drop from the peak lateral load.

5. Fragility Curves

5.1. Methodology:

As noted previously, fragility relations were developed for the ordered damage states associated with point 1 (yield) and point 2 or 3 (punching) defined in Figure 4.1 to provide the information needed to derive fragility relations for minor repair and major repair. The collected data for yielding and punching points for reinforced concrete connections without shear reinforcement are given in Table 5.1. Values for reinforced concrete specimens with shear reinforcement and post-tensioned specimens without shear reinforcement are provided in Appendix E. The four parameters given in the tables; Demand, Failure (f), Median (θ) and Dispersion (β), are defined as follows:

Demand: The value of the Demand Parameters (DPs) for the damage states. For slab-column connections, the DP for each damage state is defined as the story drift using the approach described in the prior section.

Failure (f): Condition associated with reaching or exceeding a specified damage state; 1 if reached or exceeded, otherwise, 0.

Median (θ): The outcome that is exceeded 50% of the time. In this study, the data (the demand values) are forced to follow a lognormal distribution, and x_m is the median value of the distribution of the bin that is considered. Use of a log-normal distribution is common (Tantala & Deodatis, 2002, Aslani & Miranda, 2005), and was found to reasonably fit the test data.

Dispersion (β): The logarithmic standard deviation of the distribution for a given bin.

Two fragility development methods; actual failure DP (method A) and bounding DP with damage (method B) were used to develop fragility functions (The methods are described by Porter, Kennedy and Bachman, 2007). Method A was used in cases where all of the specimens in a given bin failed at the observed values of EDP (where values of f are 1 for all specimens in a bin), whereas Method B was used in cases where some of the specimens in a bin failed (where the bin consists of specimens having f values of both 0 and 1). All of the fragility functions derived from Method A pass the Lilliefors goodness-of-fit test at the 5% significance level.

Table 5.1: Collected data for yielding and punching states for reinforced concrete specimens
without shear reinforcement

(a) $0 < V_g/V_0 < 0.2$

Specimen ID	Reference number	yielding		punching	
		demand	f	demand	f
S4	8	0.96	1	4.47	1
S5	8	0.83	1	4.03	1
AP3	28	1.2	1	5.14	1
AP4	28	1	1	3.5	1
1	9	1.27	1	4	1
2	9	1.2	1	3.16	1
A-overall	4	1.33	1	4.90	1
X_m		1.1		4	
β		0.2		0.2	

(b) $0.2 < V_g/V_0 < 0.4$

Specimen ID	Reference number	yielding		punching	
		demand	f	demand	f
1	1	0.71	1	1.54	1
3	1	1.00	1	4.52	1
ND1C	2	1.40	1	7.56	1
ND4LL	2	1.40	1	4.00	1
ND6HR	2	1.67	1	5.13	1
ND7LR	2	1.20	1	5.00	1
ND8BU	2	1.20	1	5.20	1
DNY_4	3	0.45	1	4.70	1
SC0	5	1.06	1	5.00	1
1C	6	2.00	1	3.50	1
RE-50	7	0.77	1	2.50	1
3	9	0.8	1	2.3	1
4	9	0.59	1	2.3	1
N.H.H.C.0.5	10	1.6	1	3.8	1
N.H.H.C.1.0	10	1.97	1	3.72	1
SP-Control 1	11	0.92	1	2	1
C0	12	0.77	1	1.85	1
X_m		1.1		3.6	
β		0.4		0.4	

$$(c) 0.4 \leq V_g/V_0 < 0.6$$

Specimen ID	Reference number	yielding		punching	
		demand	f	demand	f
21	13	2.93	1	4.20	1
C-02	14	1.03	1	2.40	1
C-63	14	0.83	1	2.20	1
C-overall	4	0.67	1	1.50	1
C-interior	4	0.69	1	0.70	1
ND5XL	2	1.13	1	2.00	1
CD5	16	0.57	1	1.16	1
CD8	16	0.64	1	1.38	1
SJB-7	17	1.40	1	2.38	1
X_m		0.8		1.6	
β		0.3		0.4	

5.2. Damage (Repair) States

The fragility relations for the ordered damage states were used to derive relations for the repair states. Both of the damage states and the associated repairs are summarized in Table 5.3. The process used to derive the fragility relations for Minor Repair and Major Repair are described in the following subsections.

- (i) For Minor Repair (DS1; epoxy injection of cracks), the fragility relation for yield provides a lower bound relation since yielding is required to produce residual crack widths large enough to enable epoxy injection. On the other hand, the fragility relation for the damage state associated with punching failure provides an upper bound since punching failure, in most cases, requires major repairs. To define Minor Repair, photos and sketches of crack patterns reported in the literature were reviewed and engineering judgment was used to assign a median story drift value where substantial crack lengths and residual crack widths were expected that would warrant epoxy injection (Table 5.3). It is noted that crack widths at peak loads are rarely reported in the literature and no information was reported for residual crack widths at zero lateral load (i.e., following the earthquake); therefore, documenting this type of information in future tests would be very useful. The fragility relations for Minor Repair were obtained by shifting the fragility relation for yielding to these median values. For post-tensioned connections with shear reinforcement, for which almost no data exist, DS1 (epoxy repair) fragility curves were developed based on engineering judgment by

assigning a median story drift value for each bin. The median story drift estimates of reinforced concrete specimens with shear capitals and/or drop panels were based on the only available source provided in literature (Wey and Durrani, 1992). In this test, the yielding demand value of the specimen SC6 with 24 inch shear capitals and a GSR of 0.23 was 2.4%. Given the lack of data, a median value of 2.5% was selected for drop panels and capitals with dispersion of 0.5. The resulting medians are mid-way between the relations developed for RC connections with and without shear reinforcement, respectively.

- (ii) DS2 (Major Repair) was selected to be associated with punching failure, which typically results in significant damage; therefore, the demand values and the fragility curves for DS2 (major repair) are the same as those for punching. The data for DS2 are provided in Table 5.1 for reinforced concrete specimens without shear reinforcement, and in Tables E1 and E2 (Appendix E) for reinforced concrete specimens with shear reinforcement and for post-tensioned specimens without shear reinforcement, respectively. For post-tensioned connections with shear reinforcement, for which no isolated connection test data exist, DS2 (punching) fragility curves were developed based on engineering judgment by assigning a median story drift value for each bin. Similar to what was done for yielding, the relations for shear capitals and drop panels are selected to be half-way between the relations developed for RC connections with and without shear reinforcement, respectively.

Logarithmic standard deviations (β s) of the fragility functions for connection types 4 and 5, for which no data exist, are assumed to be 0.5. Parameters of the fragility functions (θ s and β s) corresponding to the epoxy injection and major repair damage states for connection types (1), (2), and (3) are given in Table 5.4, whereas those for connection types (4) and (5) are given in Table 5.5.

The fragility relations for the two repair states are plotted in Figures 5.3 to 5.13. For reference, the fragility relations for yield also are plotted. The applicability of the functions for each bin are summarized in Table 5.2, which also provides the range of some size parameters of the specimens that were used in fragility development. Further information on various parameters is provided in Appendix A. The limits of applicability of the derived fragility curves correspond to the parameter ranges for each bin.

Table 5.2: Specimen size parameters of the bins

Bins	Slab thickness range (in)	Slab span to depth ratio
1.i	3 - 5	24 – 34
1.ii	3 - 6	13 – 34
1.iii	4.5 - 6	13 – 32
2.i	3.5 - 6	9 – 34
2.ii	4.5 - 7	25 – 32
3.i	3.5 - 5.5	18 – 40
3.ii	3.5 - 6	15 - 48

Table 5.3: Damage states and the associated repairs

Damage state	Damage state characteristics	Associated repair method	Details of repair activity
DS1	Yield strain of the slab flexural reinforcement has been exceeded, spalling of concrete may/may not occur, slab exhibits sufficiently large crack widths to allow epoxy injection.	Epoxy injection	Remove furnishings, ceilings, mechanical, electrical and plumbing systems as necessary, 5 feet either side of the damaged area. Prepare work area for epoxy injection, inject epoxy, and replace and repair finishes. Replace furnishings, ceilings, mechanical, electrical, and plumbing systems. Length of cracks to be injected for each type of connection is provided in Table 6.1.
DS2	Slab punching failure occurs, causing significant spalling of concrete. Epoxy injection is no longer expected to be sufficient to restore the required strength and stiffness to the slab and the slab-column connection.	Major repair	<p>Remove furnishings, ceilings, mechanical, electrical and plumbing systems as necessary, 15 feet either side of the damaged area. Shore damaged area a minimum of one level below (more levels if necessary). Remove damaged concrete at least 1 inch beyond the exposed reinforcing steel. Place concrete forms, and then concrete. Remove forms, replace and repair finishes. Replace furnishings, ceilings, mechanical, electrical, and plumbing systems.</p> <p>Significant drop of the slab relative to column would be expected; 1) if no shear reinforcement is provided, and 2) if the slab punches outside the shear reinforced zone. Illustration to this can be seen in Figure 5.1 for Type 1 connections and in Figure 5.2 for Type 3 connections. This case requires floor leveling prior to major repair (and more shoring), and slab flexural reinforcement may need to be removed, and new reinforcement spliced to existing reinforcement.</p>

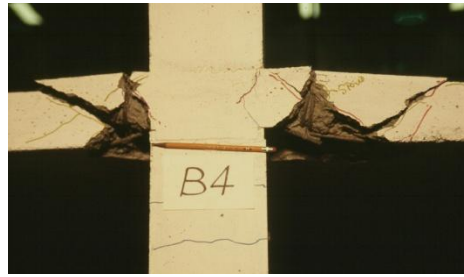


Figure 5.1: Punching failure for RC connection without shear reinforcement with significant drop in floor slab – major repair required [Hwang and Moehle, 1989]



Figure 5.2: Punching failure for PT connection without shear reinforcement with significant drop in floor slab – major repair required [Kang , 2006]

Instead of providing the same fragility curves for reinforced concrete connections with shear capitals/drop panels (type 5) as the curves for reinforced concrete specimens with/without shear reinforcement (type 1 or 2), fragility functions for type 5 connections were derived using engineering judgment. The main reason for the derivation is that addition of shear capitals/drop panels increases the drift capacity of the connections (Wey & Durrani, 1992); however, the improvement, based on the limited test data, is not as significant as if shear reinforcement is provided. Thus, the median drift value for type 5 connections was assigned a value approximately at mid-way of the median values for type 1 and type 2 connections.

Table 5.4: Parameters of the fragility functions for connection types 1, 2, and 3

(a) Reinforced Concrete Specimens without Shear Reinforcement, $0 < V_g/V_0 < 0.2$

Parameters	DS1	DS2
x_m	2.5	4.0
β	0.4	0.4

(b) Reinforced Concrete Specimens without Shear Reinforcement, $0.2 < V_g/V_0 < 0.4$

Parameters	DS1	DS2
x_m	2.0	3.5
β	0.4	0.4

(c) Reinforced Concrete Specimens without Shear Reinforcement, $0.4 \leq V_g/V_0 < 0.6$

Parameters	DS1	DS2
x_m	1.2	1.5
β	0.4	0.4

(d) Reinforced Concrete Specimens with Shear Reinforcement, $0.2 < V_g/V_0 < 0.4$

Parameters	DS1	DS2
x_m	3.0	4.8
β	0.4	0.5

(e) Reinforced Concrete Specimens with Shear Reinforcement, $0.4 \leq V_g/V_0 < 0.6$

Parameters	DS1	DS2
x_m	2.2	3.0
β	0.4	0.5

(f) Post-Tensioned Specimens without Shear Reinforcement, $0.2 < V_g/V_0 < 0.4$

Parameters	DS1	DS2
x_m	1.8	3.0
β	0.4	0.4

(g) Post-Tensioned Specimens without Shear Reinforcement, $0.4 < V_g/V_0 < 0.6$

Parameters	DS1	DS2
x_m	1.25	1.9
β	0.4	0.5

Table 5.5: Parameters of the fragility functions for connection types 4 and 5

(a) Post-Tensioned Specimens with Shear Reinforcement, $0.2 < V_g/V_0 < 0.4$

Parameters	DS1	DS2
x_m	2.8	4.0
β	0.5	0.5

(b) Post-Tensioned Specimens with Shear Reinforcement, $0.4 < V_g/V_0 < 0.6$

Parameters	DS1	DS2
x_m	2.3	3.2
β	0.5	0.5

(c) Reinforced Concrete Specimens with Shear Capitals/Drop Panels, $0.2 < V_g/V_0 < 0.4$

Parameters	DS1	DS2
x_m	2.5	4.2
β	0.5	0.5

(d) Reinforced Concrete Specimens with Shear Capitals/Drop Panels, $0.4 < V_g/V_0 < 0.6$

Parameters	DS1	DS2
x_m	1.7	2.3
β	0.5	0.5

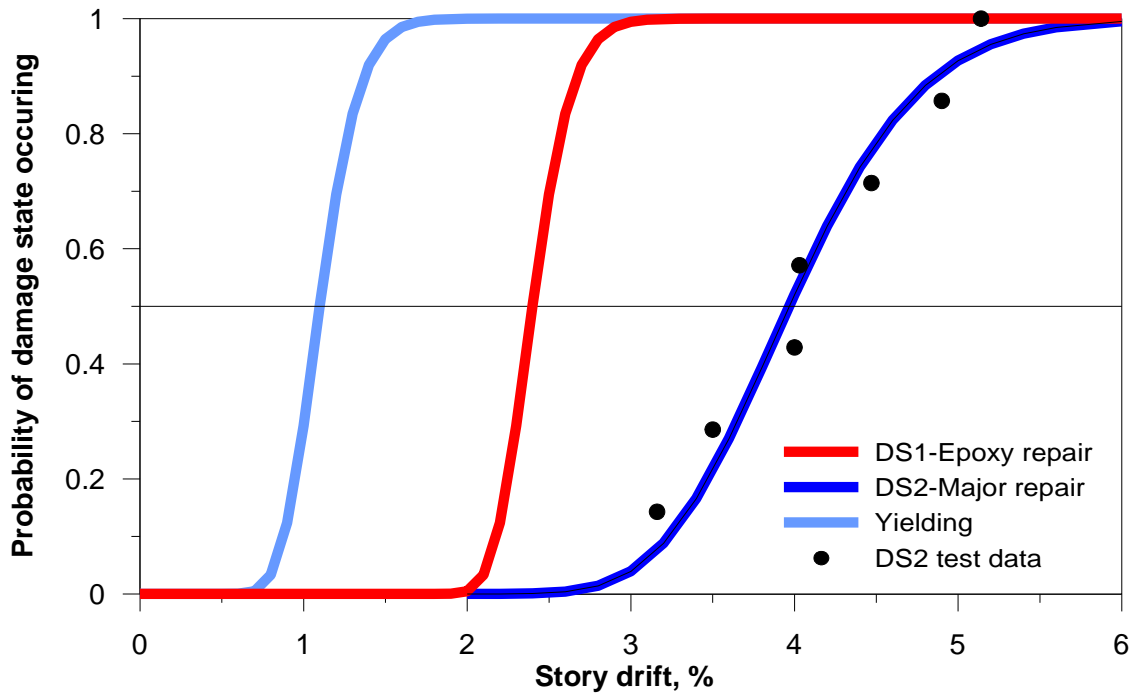


Figure 5.3: Fragility curves for RC connections without shear reinforcement,
 $0 \leq \text{GSR} < 0.2$

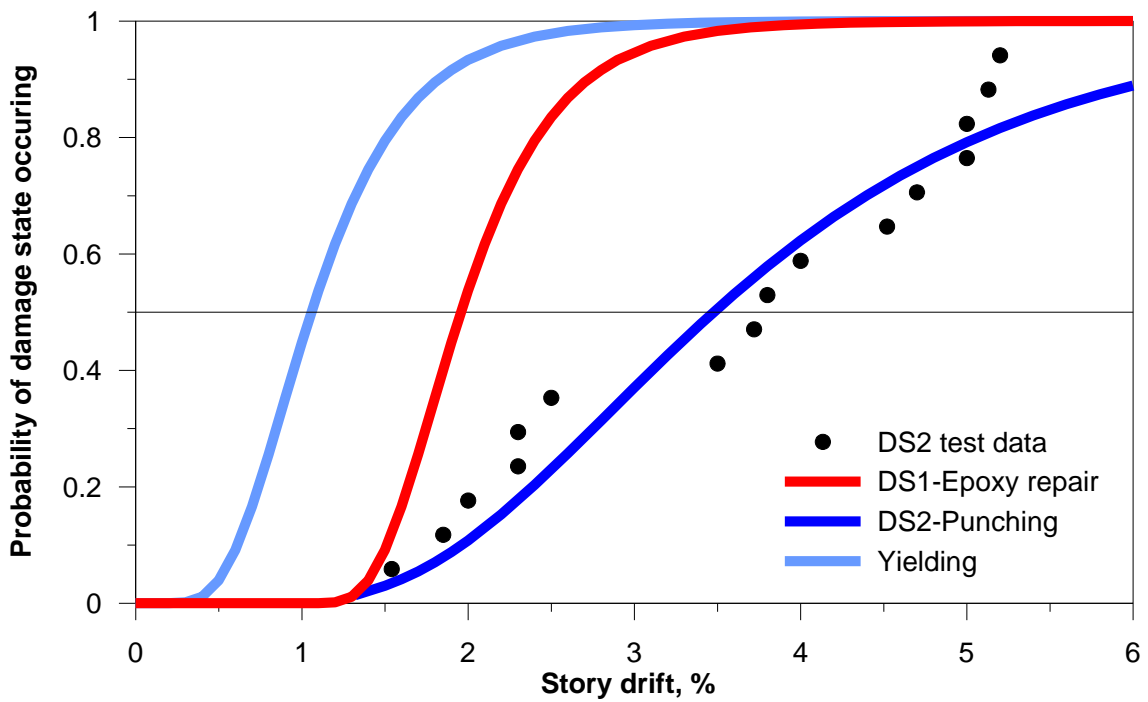


Figure 5.4: Fragility curves for RC connections without shear reinforcement,
 $0.2 \leq \text{GSR} < 0.4$

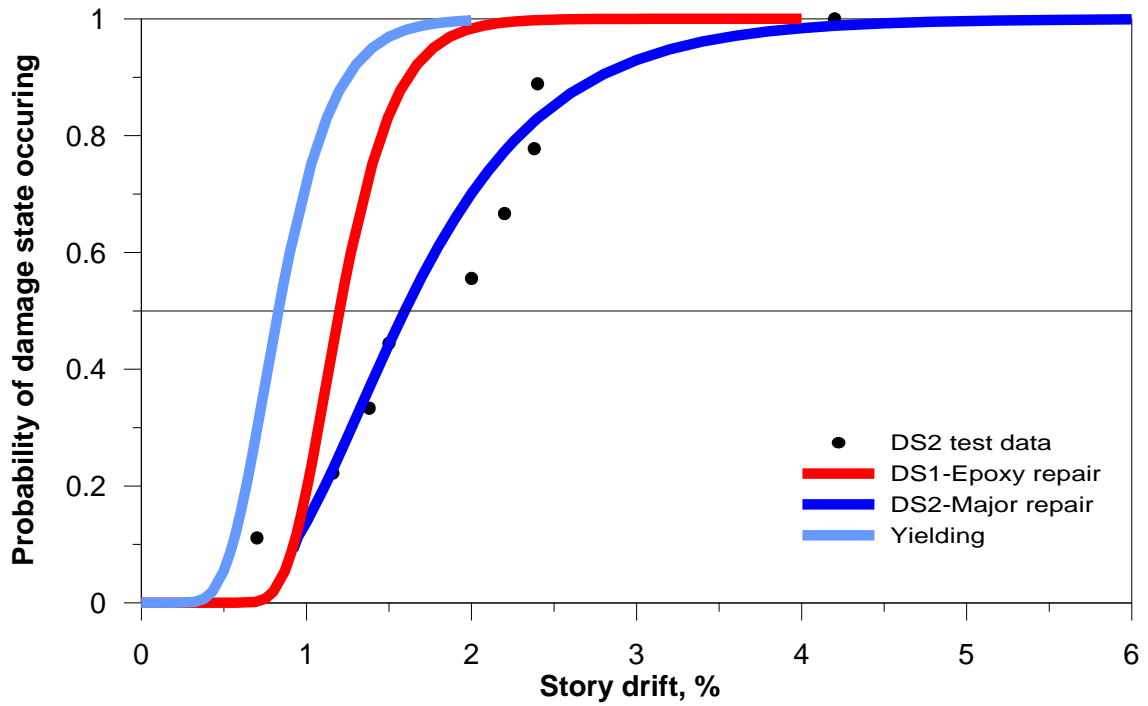


Figure 5.5: Fragility curves for RC connections without shear reinforcement,
 $0.4 \leq \text{GSR} < 0.6$

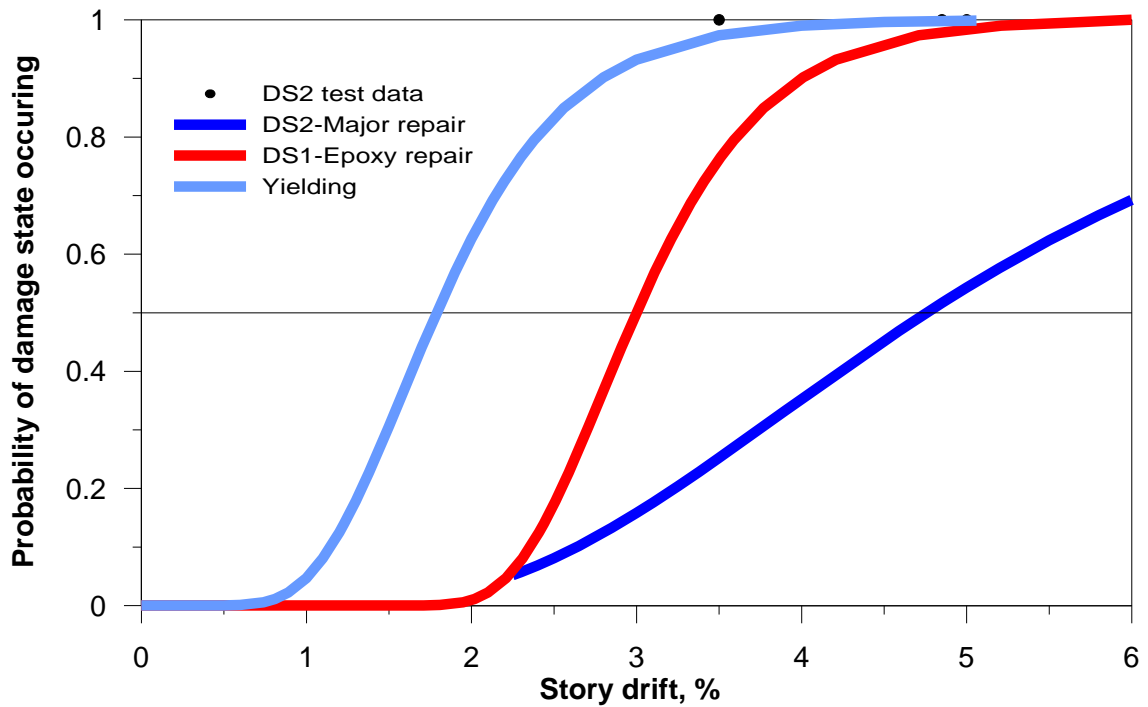


Figure 5.6: Fragility curves for RC connections with shear reinforcement,
 $0 \leq \text{GSR} < 0.2$ & $0.2 \leq \text{GSR} < 0.4$

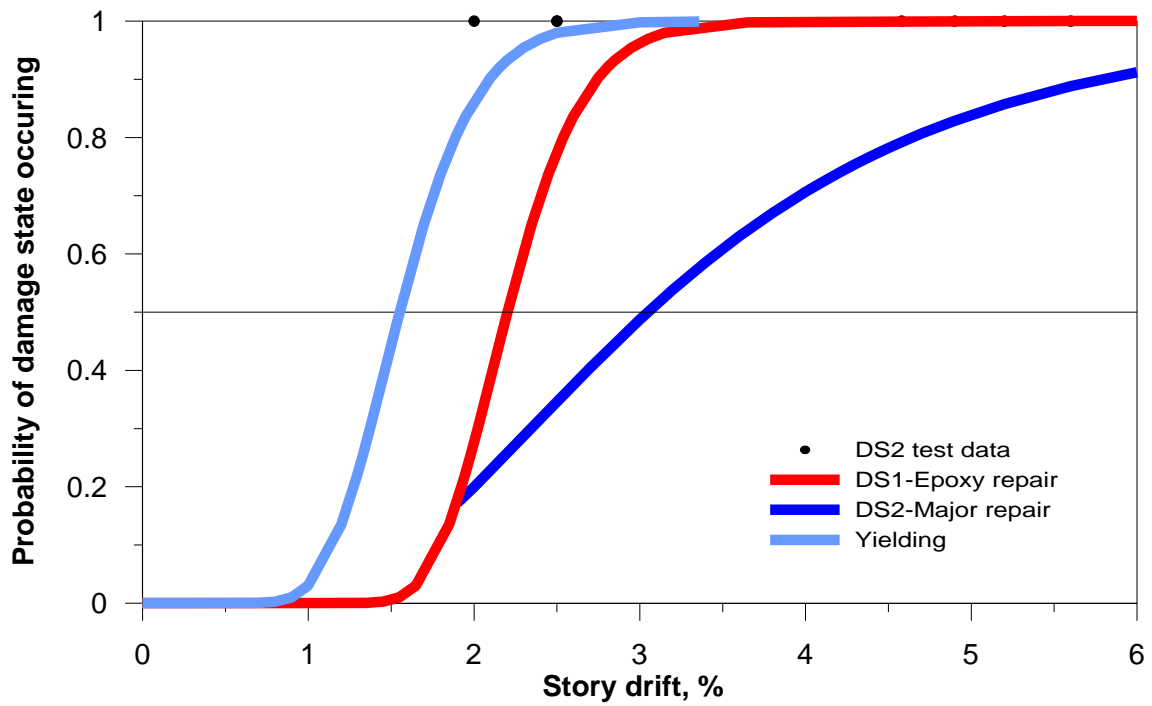


Figure 5.7: Fragility curves for shear RC connections with shear reinforcement,
 $0.4 \leq \text{GSR} < 0.6$

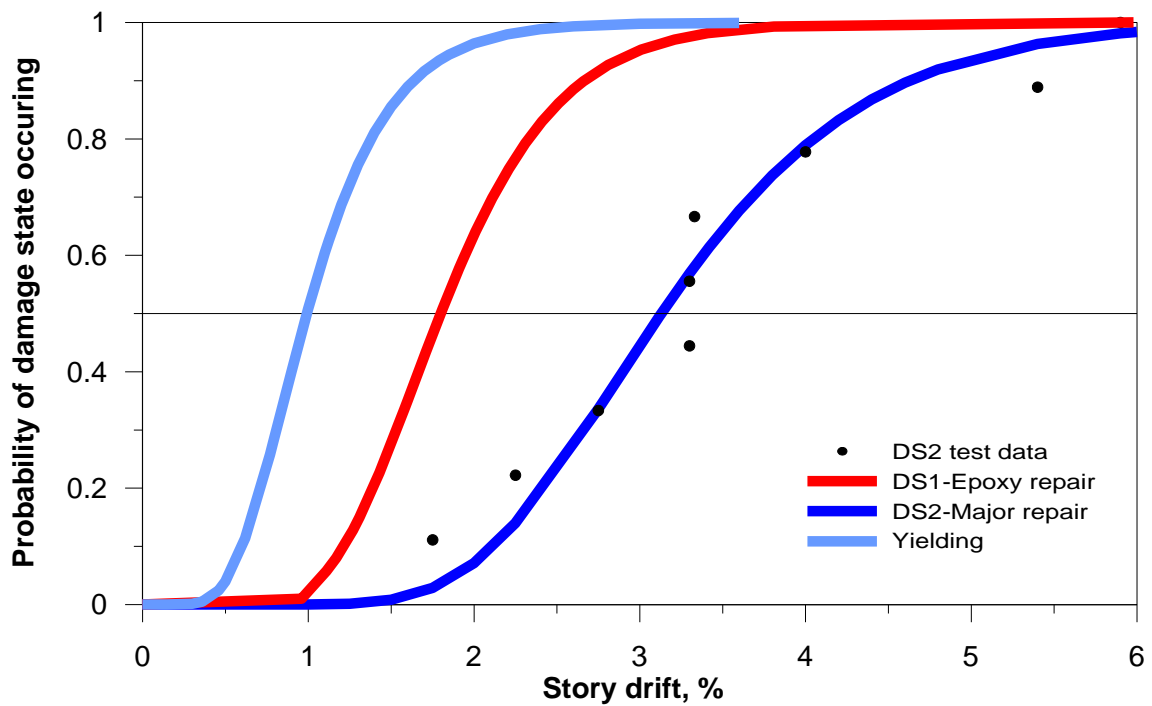


Figure 5.8: Fragility curves for PT connections without shear reinforcement,
 $0 \leq \text{GSR} < 0.2$ & $0.2 \leq \text{GSR} < 0.4$

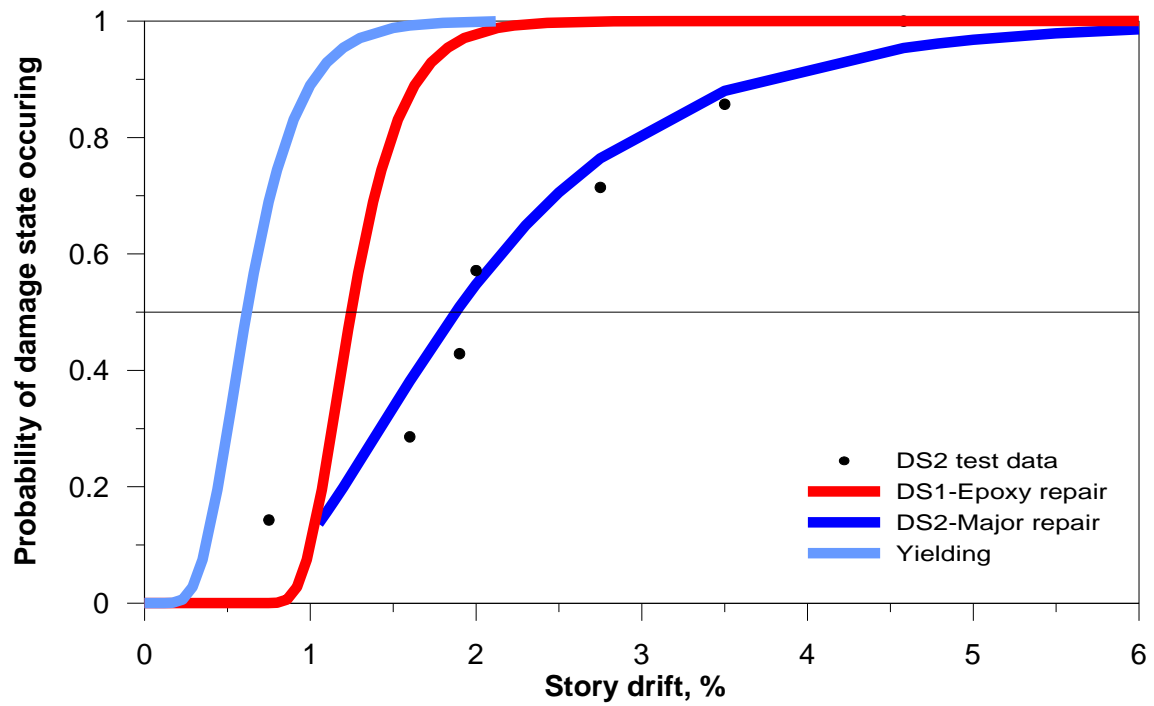


Figure 5.9: Fragility curves for PT connections without shear reinforcement,
 $0.4 \leq \text{GSR} < 0.6$

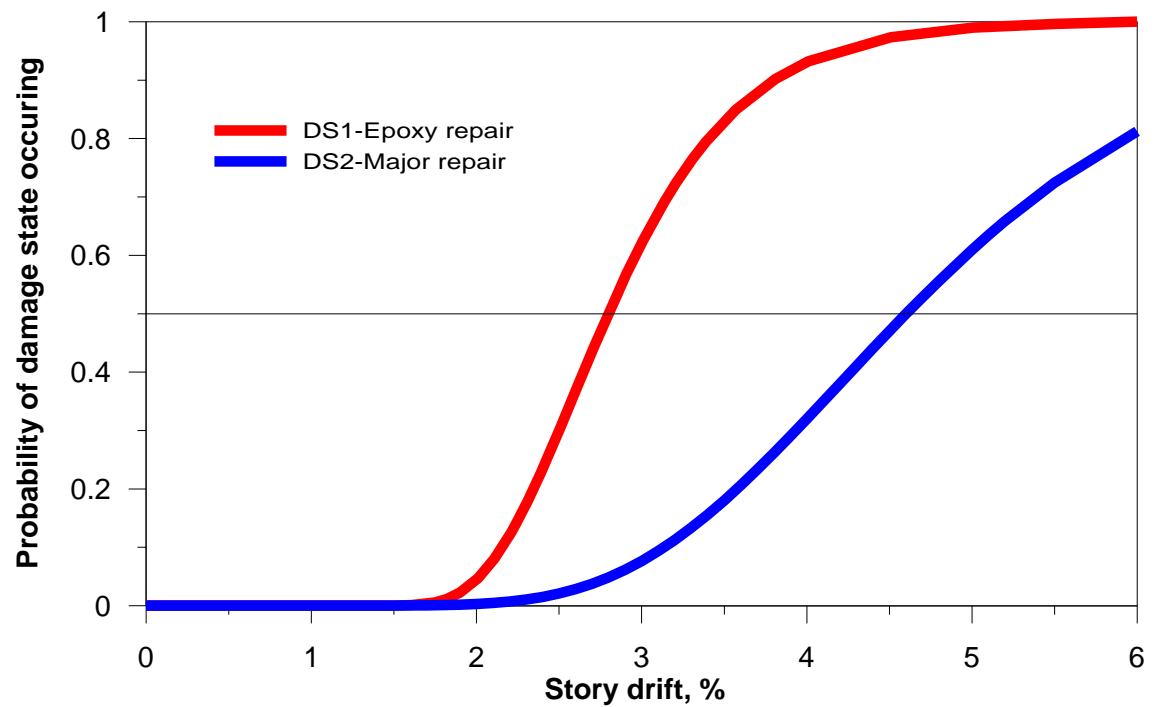


Figure 5.10: Fragility curves for shear reinforced PT connections,
 $0 \leq \text{GSR} < 0.2$ & $0.2 \leq \text{GSR} < 0.4$

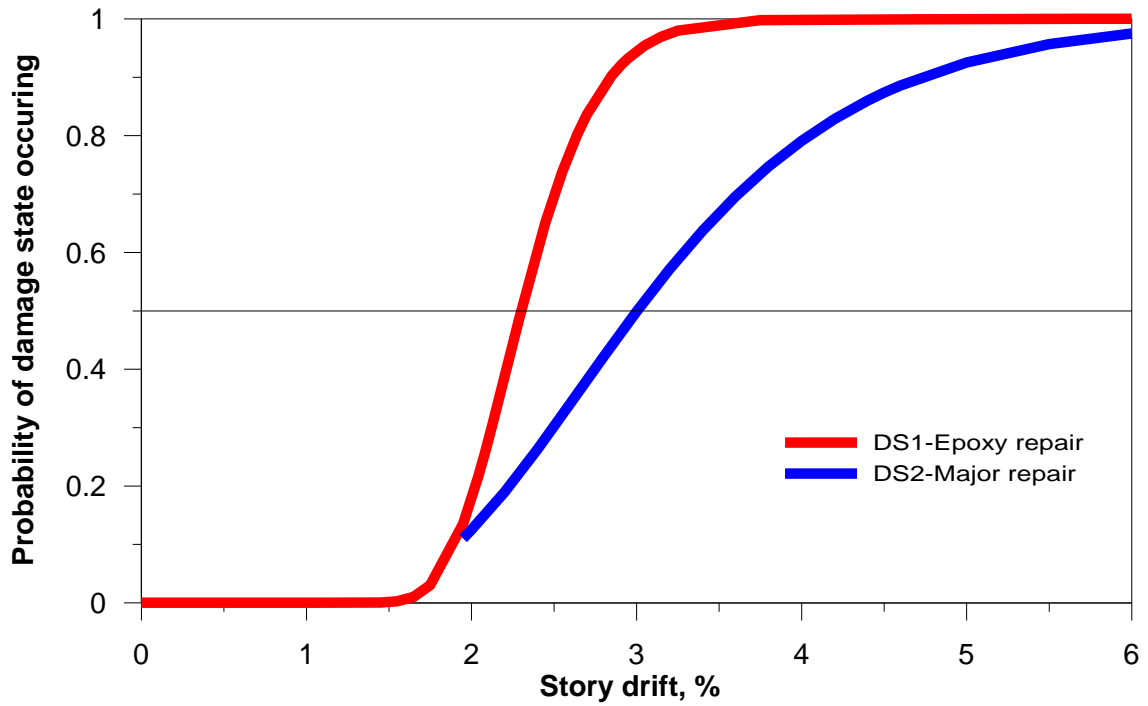


Figure 5.11: Fragility curves for shear reinforced PT connections,
 $0.4 \leq \text{GSR} < 0.6$

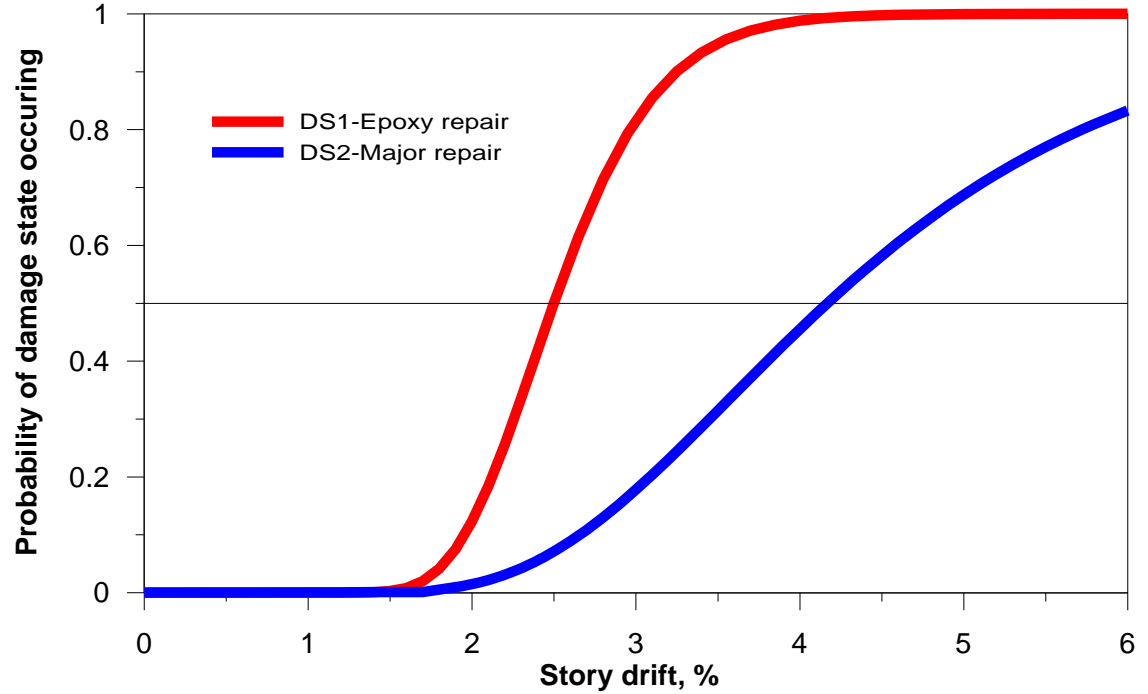


Figure 5.12: Fragility curves for RC connections with shear capitals/drop panels,
 $0 \leq \text{GSR} < 0.2$ & $0.2 \leq \text{GSR} < 0.4$

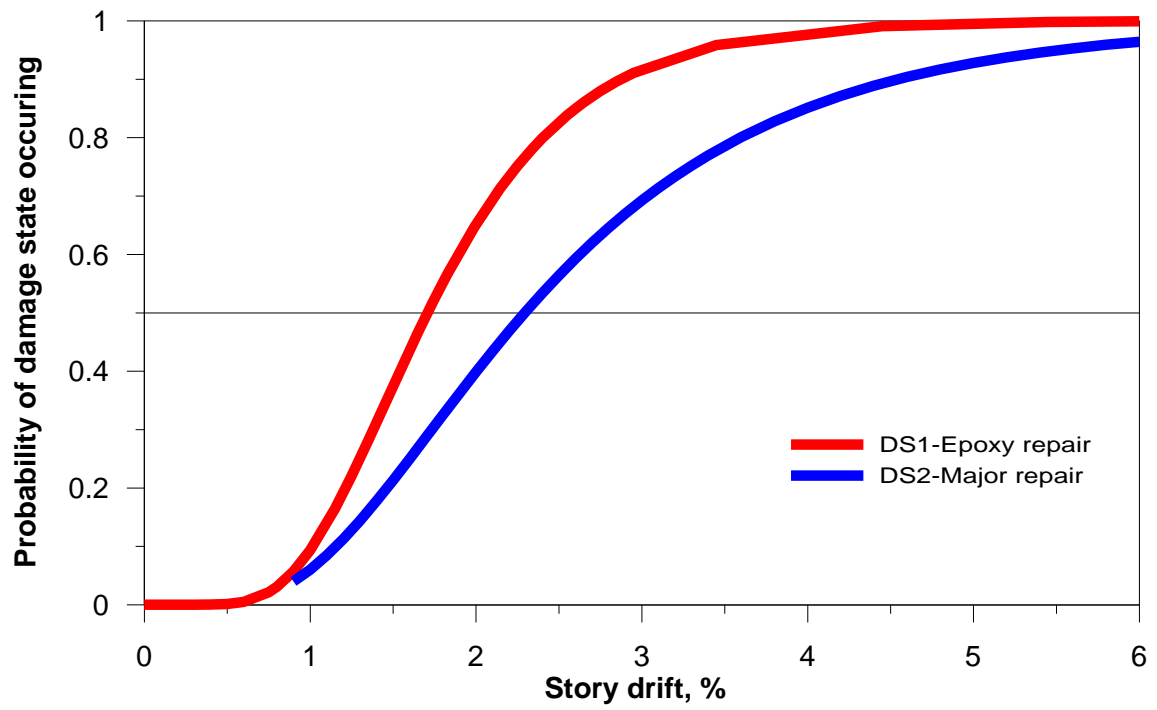


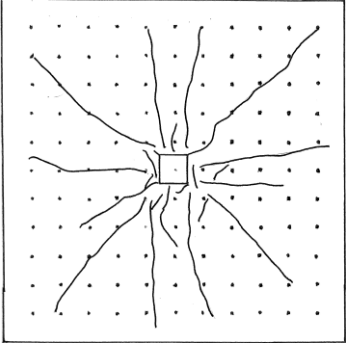
Figure 5.13: Fragility curves for RC connections with shear capitals/drop panels,
 $0.4 \leq \text{GSR} < 0.6$

6. Crack Patterns and Images

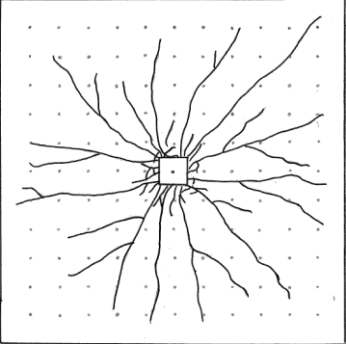
No crack patterns or images for DS1 (Minor Repair) are available in the literature. While most researchers report crack patterns for DS2, relatively few report crack patterns for drift values prior to punching. Therefore, it was necessary to estimate DS1 crack patterns for each bin by adjusting the available crack patterns reported at punching failure (DS2) to median drift values associated with DS1. The crack patterns and lengths are given in Table 6.1 for DS1 and Table 6.2 for DS2. Total crack lengths were first estimated from the test specimens, which are typically about one-half scale (test slab dimensions of 12.5 ft x 12.5 ft, or $\approx 160 \text{ ft}^2$). Cracks lengths for full-scale slab panels were determined from the test panels as: $L_{cr} = (L_p^2) L_{ct} / (12.5)^2 = (L_p^2) L_{ct} / 160$, where L_{ct} is the total crack length estimated from the test specimens, 160 is the area of the test panel in square feet, L_p is the length of the sides of the full-scale square panel, and L_{cr} is the resulting estimate of the total crack length for a full-scale connection. Results reported in Table 6.1 and 6.2 represent full-scale slab panels assuming reinforced concrete slab panels of 22 ft x 22 ft and post-tensioned slab panels of 30 ft x 30 ft. Total crack lengths of slabs having dimensions other than 22 ft x 22 ft (RC) and 30 ft x 30 ft (PT), can be calculated using the same equation (with a different denominator). Due to the lack of data, no crack patterns or images are available for connection types of c and d, or for reinforced concrete specimens without shear reinforcement having GSR values less than 0.2.

Table 6.1: Crack patterns of DS1

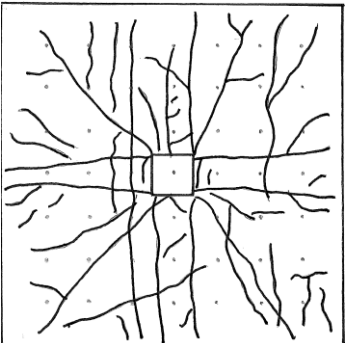
(a) Reinforced Concrete Specimens without Shear Reinforcement, $0.0 < V_g/V_0 < 0.4$

	<p>Total crack length (based on slab dimensions of 22ftx22ft) :</p> <p>180 ft</p>
---	---

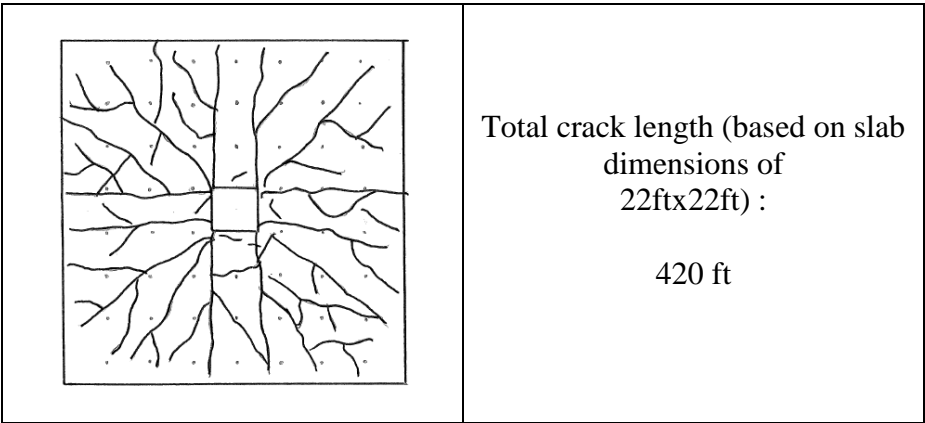
(b) Reinforced Concrete Specimens without Shear Reinforcement, $0.4 \leq V_g/V_0 < 0.6$

	<p>Total crack length(based on slab dimensions of 22ftx22ft) :</p> <p>270 ft</p>
--	--

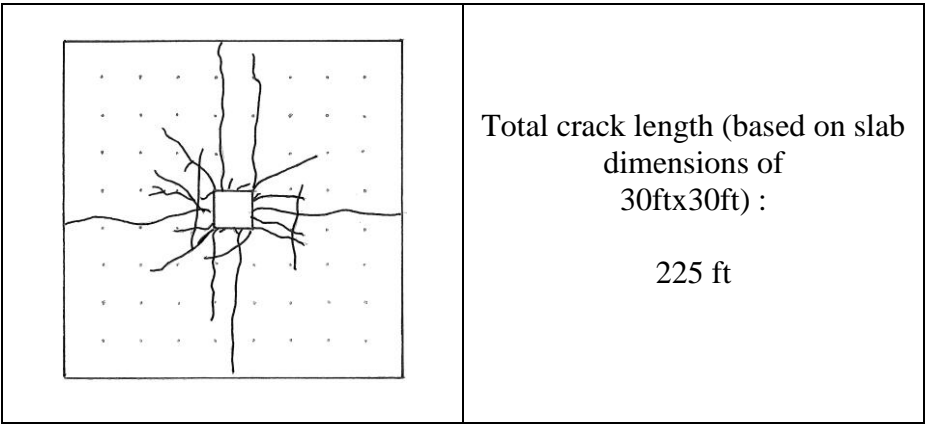
(c) Reinforced Concrete Specimens with Shear Reinforcement, $0.2 < V_g/V_0 < 0.4$

	<p>Total crack length (based on slab dimensions of 22ftx22ft) :</p> <p>345 ft</p>
---	---

(d) Reinforced Concrete Specimens with Shear Reinforcement, $0.4 \leq V_g/V_0 < 0.6$



(e) Post-Tensioned Specimens without Shear Reinforcement, $0.2 < V_g/V_0 < 0.4$



(f) Post-Tensioned Specimens without Shear Reinforcement, $0.4 < V_g/V_0 < 0.6$

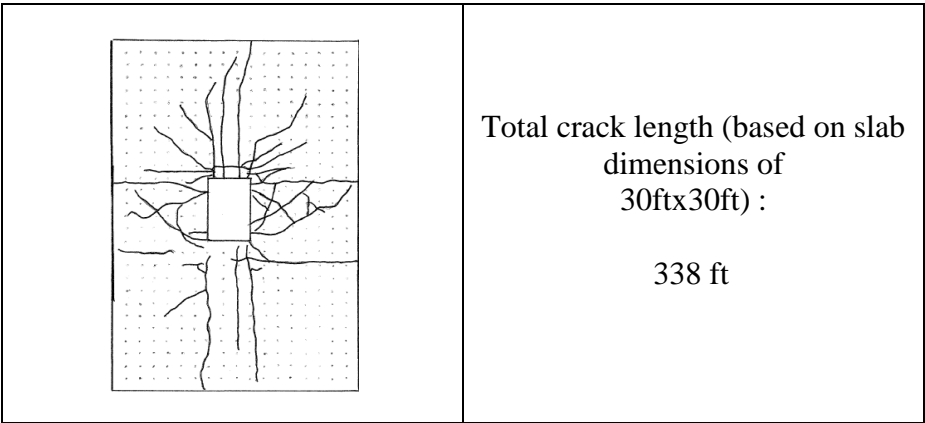
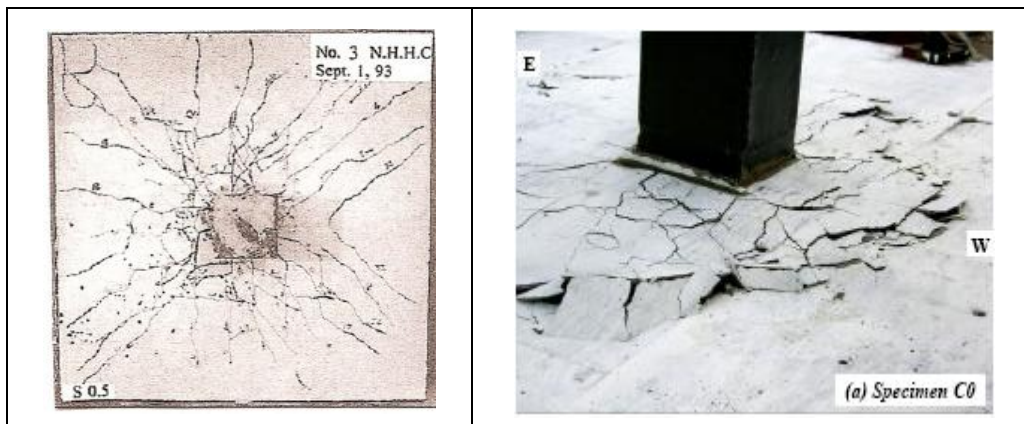
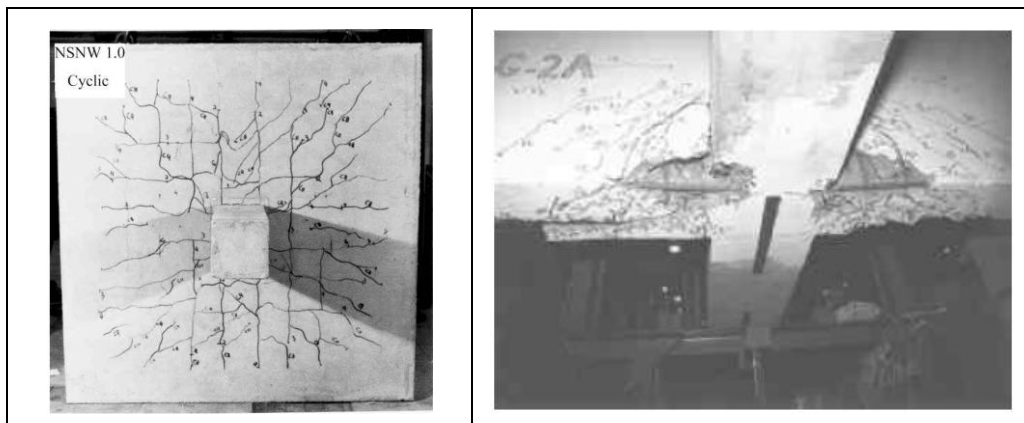


Table 6.2: Crack patterns and images of DS2

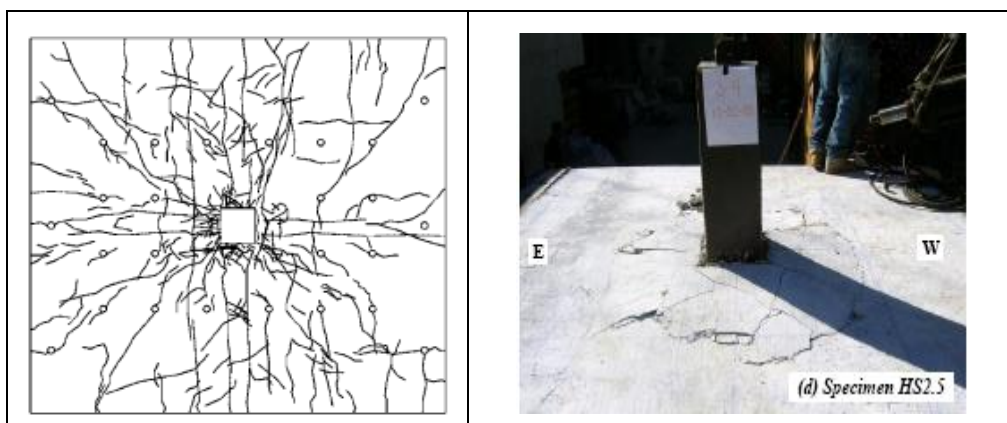
(a) Reinforced Concrete Specimens without Shear Reinforcement, $0.2 < V_g/V_0 < 0.4$



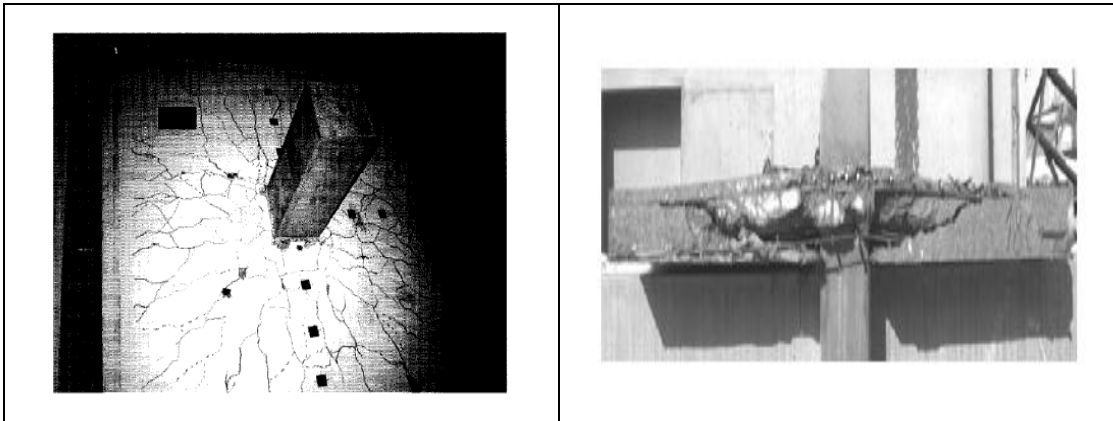
(b) Reinforced Concrete Specimens without Shear Reinforcement, $0.4 \leq V_g/V_0 < 0.6$



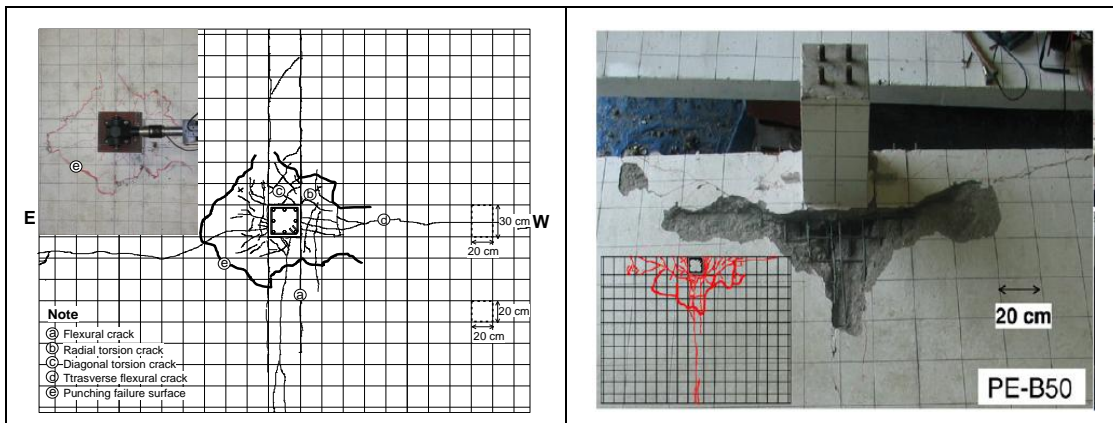
(c) Reinforced Concrete Specimens with Shear Reinforcement, $0.2 < V_g/V_0 < 0.4$



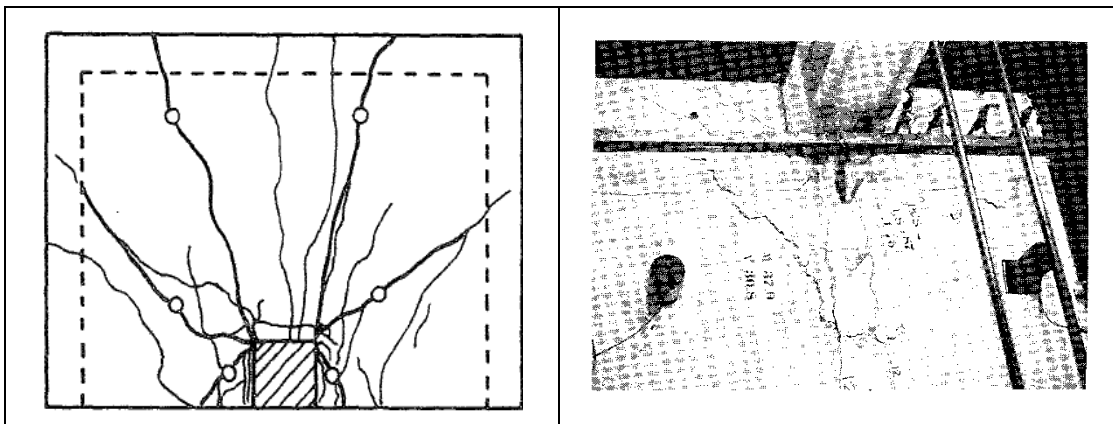
(d) Reinforced Concrete Specimens with Shear Reinforcement, $0.4 \leq V_g/V_0 < 0.6$



(e) Post-Tensioned Specimens without Shear Reinforcement, $0.2 < V_g/V_0 < 0.4$



(f) Post-Tensioned Specimens without Shear Reinforcement, $0.4 < V_g/V_0 < 0.6$



References

1. Pan, A., and Moehle, J.P., "An Experimental Study of Slab-Column Connections", *ACI Structural Journal*, V. 89, No. 6, November-December 1992, pp. 626-638.
2. Robertson, I., and Johnson, G., "Cyclic Lateral Loading of Nonductile Slab-Column Connections", *ACI Structural Journal*, V. 103, No. 3, May-June 2006, pp. 356-364.
3. Durrani, A. J., Du, Y., and Luo, Y. H., "Seismic Resistance of Nonductile Slab-Column Connections in Existing Flat-Slab Buildings", *ACI Structural Journal*, V. 92, No. 4, July-August 1995, pp. 479-487.
4. Roberson, I. N., and Durrani, A. J., "Gravity Load Effect on Seismic Behaviour of Interior Slab-Column Connections", *ACI Structural Journal*, V. 89, No. 1, January-February 1992, pp. 37-45.
5. Wey, E. H., and Durrani, A. J., "Seismic Response of Interior Slab-Column Connections with Shear Capitals", *ACI Structural Journal*, V. 89, No. 6, November-December 1992, pp. 682-691.
6. Robertson, I. N., Kawai, T., Lee, J., and Enomoto, B., "Cyclic Testing of Slab-Column Connections with Shear Reinforcement", *ACI Structural Journal*, V. 99, No. 5, September-October 2002, pp. 605-613.
7. Han, S. W., Kee, S., Park, Y., Lee, L., and Kang, T. H., "Hysteretic Behavior of Exterior Posit-Tensioned Flat Plate Connections", 2006.
8. Morrison, D. G., Hirasawa, I., and Sozen, M. A., "Lateral-Load Tests of R/C Slab-Column Connections", *Journal of Structural Engineering*, Vol. 109, No. 11, November 1983, pp. 2698-2714.
9. Farhey, D. N., Adin, M., A., and Yankelevsky, D. Z., "RC Flat Slab-Column Subassemblages under Lateral Loading", *Journal of Structural Engineering*, Vol. 119, No. 6, June 1993, pp. 1903-1916.
10. Emam, M., Marzouk, H., Hilal, M. S., "Seismic Response of Slab-Column Connections Constructed with High-Strength Concrete", *ACI Structural Journal*, V. 94, No. 2, March-April 1997, pp. 197-205.
11. Widiyanto, Tian, Y., Argudo, J., Bayrak, O., Jirsa, J. O., "Rehabilitation of Earthquake-Damaged Reinforced Concrete Flat-Plate Slab-Column Connections for Two-Way Shear", *Proceedings of the 8th U.S. National Conference on Earthquake Engineering*, San Francisco, California, USA, 2006.
12. Kang, T. H., and Wallace, J. W., "Seismic Performance of Reinforced Concrete Slab-Column Connections with Thin Plate Stirrups", 2008.
13. Marzouk, H., Osman, M., and Hussein, A., "Cyclic Loading of High-Strength Lightweight Concrete Slabs", *ACI Structural Journal*, V. 98, No. 2, March-April 2001, pp. 207-214.
14. Stark, A., Binici, B., and Bayrak, O., "Seismic Upgrade of Reinforced Concrete Slab-Column Connections Using Carbon Fiber-Reinforced Polymers", *ACI Structural Journal*, V. 102, No. 2, March-April 2005, pp. 324-333.

15. Megally, S., and Ghali, A., "Seismic Behavior of Edge Column-Slab Connections with Stud Shear Reinforcement", *ACI Structural Journal*, V. 97, No. 1, January-February 2000, pp. 53-61.
16. Cao, H., "Seismic Design of Slab-Column Connections", PhD thesis, The University of Calgary, February 1993.
17. Brown, S. J., "Seismic Response of Slab-Column Connections", PhD thesis, The University of Calgary, April 2003.
18. Islam, S., and Park, R., "Tests on Slab-Column Connections with Shear and Unbalanced Flexure", *ASCE Journal of Structural Division*, V. 102, No. ST3, March 1976, pp. 549-568.
19. Broms, C. E., "Flat Plates in Seismic Areas: Comparison of Shear Reinforcement Systems", *ACI Structural Journal*, V. 104, No. 6, November-December 2007, pp. 712-721.
20. Trongtham, N., and Hawkins, N. M., "Moment Transfer to Columns in Unbonded Post-Tensioned Prestressed Concrete Slabs", *Report SM77-3*, Department of Civil Engineering, University of Washington-Seattle, WA, 1977, 186 pp.
21. Martinez-Cruzado, J. A., "Experimental Study of Post-Tensioned Flat Plate Exterior Slab-Column Connections Subjected to Gravity and Biaxial Loading", PhD thesis, Department of Civil Engineering, University of California-Berkeley, Berkeley, CA, 1993, 303 pp.
22. Kang, T. H., Kee, S-H., Han, S. W., Lee, L-H., and Wallace, J. W., "Interior Post-Tensioned Slab-Column Connections Subjected to Cyclic Lateral Loading", *Proceedings of the 8th U.S. National Conference on Earthquake Engineering*, San Francisco, California, USA, 2006.
23. Dilger, W. H., and Shatila, M., "Shear Strength of Prestressed Concrete Edge Slab-Column Connections with and without Shear Stud Reinforcement", MsC thesis, University of Calgary, 1987.
24. Qaisrani, A.-N., "Interior Post-Tensioned Flat-Plate Connections Subjected to Vertical and Biaxial Lateral Loading", PhD thesis, Department of Civil Engineering, University of California-Berkeley, Berkeley, CA, 1993, 303 pp.
25. Pimanmas, A., Warnitchai, P., and Pongpornsup, S., "Seismic Performance of 3/5 Scaled Post-Tensioned Interior Flat Slab-Column Connections", *Proceedings of the Asi Conference on Earthquake Engineering 2004*, Manila, Philippines, March 2004, 9 pp.
26. Han, S-W., Kee, S-H., Ha, S-S., and Wallace, J. W., "Effects of Bottom Reinforcement on Hysteretic Behavior of Post-Tensioned Flat Plate Connections", 2008
27. REMR Technical Note CS-MR-3.9, "Crack Repair Method: Epoxy Injection"
28. Pan, A., and Moehle, J.P., "Lateral Displacement Ductility of Reinforced Concrete Flat Plates", *ACI Structural Journal*, V. 86, No. 3, May-June 1989, pp. 250-258.

29. Porte, K. A., R. P. Kennedy, and R. E. Bachman,. “Creating fragility functions for performance based earthquake engineering”, *Earthquake Spectra*, V.23, No.2, May 2007, pp. 471-489.
30. Tantala, M. W., Deodatis, G., “Development of Seismic Fragility Curves for Tall Buildings”, ASCE Engineering Mechanics Conference, June 2-5, Columbia University, New York.
31. Aslani, H., and Miranda, E., “Fragility Assessment of Slab-Column Connections in Existing Non-ductile Reinforced Concrete Buildings”, *Journal of Earthquake Engineering*, V.9, No. 6, 2005, pp, 777-804.

Appendices

A. Spreadsheet with data collected from test reports

Table A1: Reinforced concrete specimens without shear reinforcement, $0 \leq \text{GSR} < 0.2$

Specimen ID	Authors (Referred to the references)	GSR	Test configuration	Slab size (in _x in _x in)	Span to depth ratio	fc' as tested (psi)	Column size (in)	f _y as tested (ksi)	Maximum drift, %	Code
A-overall	4	0.18	2 span	114x78x4.5	25.3	4790	10x10x60.5	72.6	5	ACI 318-83
S5	8	0.17	interior	72x72x3	24	5104	12x12x44	49.3	5.4	ACI 318-77
S4	8	0.08	interior	72x72x3	24	5062	12x12x44	46.4	5.4	ACI 318-77
AP3	28	0.18	interior	144x144x4.8	30	4600	10.8x10.8x72	70.2	3.7	ACI 318-83
AP4	28	0.19	interior	144x144x4.8	30	4500	10.8x10.8x72	70.2	3.5	ACI 318-83
1	9	0	Interior	106x106x3.15	33.6	5089	11.8x7.9x62	41&66	4.75	ACI 318-89
2	9	0	interior	106x106x3.15	33.6	5089	11.8x7.9x62	41&66	3.8	ACI 318-89

Table A2: Reinforced concrete specimens without shear reinforcement, $0.2 \leq \text{GSR} < 0.4$

Specimen ID	Authors (Referred to the references)	GSR	Test configuration	Slab size (in x in x in)	Span to depth ratio	fc' as tested (psi)	Column size (in)	f _y as tested (ksi)	Maximum drift, %	Code
1	1	0.35	interior	144x144x4.8	30	4825	10.8x10.8x85.7	68.4	2.63	ACI 318-89
3	1	0.22	interior	144x144x4.8	30	4550	10.8x10.8x85.7	68.4	4.76	ACI 318-89
ND1C	2	0.25	interior	120x108x4.5	26.7	4292	10x10x54	58	8	ACI 318-63
ND4LL	2	0.37	interior	120x108x4.5	26.7	4684	10x10x54	58	5	ACI 318-63
ND6HR	2	0.30	interior	120x108x4.5	26.7	3814	10x10x54	58	5	ACI 318-63
ND7LR	2	0.36	interior	120x108x4.5	26.7	2726	10x10x54	58	5	ACI 318-63
ND8BU	2	0.24	interior	120x108x4.5	26.7	5684	10x10x54	58	5	ACI 318-63
DNY_4	3	0.28	2 span	114x78x4.5	25.3	2772	10x10x60.6	54	5.57	ACI 318-56
SC0	5	0.23	interior	114x78x4.5	25.3	5799	10x10x(not given)	76.13	5	ACI-318-89
1C	6	0.25	interior	118x21.6x4.5	26	5133	9.84x9.84x60	60.9	4	ACI-318-99
RE-50	7	0.37	exterior	94.5x141.7x5.1	18.5	4684	11.8x11.8x82	67.57	2.5	ACI-318-05
3	9	0.25	interior	106x106x3.15	33.65	1752	7.9x11.8x62.2	41 & 66.35	3.2	ACI 318-89
4	9	0.25	interior	106x106x3.15	33.75	1752	4.7x11.8x62.2	41 & 66.35	3.2	ACI 318-89
N.H.H.C.0.5	10	0.33	interior	74.8x74.8x5.9	12.68	5330	9.8x9.8x73.6	66.7	3.9	ACI 318-95
N.H.H.C.1.0	10	0.36	interior	74.8x74.8x5.9	12.68	5129	9.8x9.8x73.6	66.7	3.6	ACI 318-95
SP-Control 1	11	0.23	interior	168x168x6	28	3710	16x16x96	63 & 66	2.5	ACI 318-05
C0	12	0.33	interior	120x120x6	20	5597	9.8x9.8x72	65.5	5	ACI-318-05

Table A3: Reinforced concrete specimens without shear reinforcement, $0.4 \leq \text{GSR} < 0.6$

Specimen ID	Authors (Referred to the references)	GSR	Test configuration	Slab size (in x in x in)	Span to depth ratio	fc' as tested (psi)	Column size (in)	f _y as tested (ksi)	Maximum drift, %	Code
21	13	0.41	interior	74.8x74.8x5.9	12.67	≈ 5075	9.8x9.8x72.8	min. 58	5.3	ACI-318-99
C-02	14	0.4	interior	112x112x4.5	25	4480	W10x88, h=64.3	65.8	4	ACI-318-02
C-63	14	0.4	interior	112x112x4.5	25	4480	W10x88, h=64.3	65.8	2.5	ACI-318-63
C-overall	4	0.51	2 span	114x78x4.5	25.3	4670	10x10x60.5	76.1	2	ACI 318-83
C-interior	4	0.51	interior	114x78x4.5	25.3	4670	10x10x60.5	76.1	2	ACI 318-83
ND5XL	2	0.47	interior	120x108x4.5	26.7	3495	10x10x54	58	2	ACI-318-63
CD5	16	0.53	interior	74.8x74.8x5.9	32	4524	9.8x9.8x55.5	57.3	0.71	CAN3-A23.2-M84
CD8	16	0.42	interior	74.8x74.8x5.9	32	3915	9.8x9.8x55.5	57.3	1.42	CAN3-A23.2-M84
SJB-7	17	0.56	interior	74.8x74.8x5.9	32	4176	9.8x9.8x54.7	57.3	2.4	A23.3 & MC-90

Table A4: Reinforced concrete specimens with shear reinforcement, $0.2 \leq \text{GSR} < 0.4$

Specimen ID	Authors (Referred to the references)	GSR	Test configuration	Slab size (in x in x in)	Span to depth ratio	fc' as tested (psi)	Column size (in)	Shear reinforcement type	Flexural reinf. actual f _y (ksi)	Shear reinf. actual f _y (ksi)
2CS	6	0.27	interior	118x108x4.5	26	4553	9.8x9.8x60	closed stirrups	61	67.4
3SL	6	0.23	interior	118x108x4.5	26	6293	9.8x9.8x60	single leg stirrups	61	67.4
4HS	6	0.24	interior	118x108x4.5	26	5539	9.8x9.8x60	headed studs	61	67.4
MG-5	15	0.31	edge	53.2x74x6	8.9	4098	10x10x55	headed studs	78.3	not specified
6CS	18	0.24	interior	120x90x3.5	34.2	4090	9x9x60	closed stirrups	42.1	54.8
7CS	18	0.24	interior	120x90x3.5	34.2	4310	9x9x60	closed stirrups	44.1	53
8CS	18	0.27	interior	120x90x3.5	34.2	3210	9x9x60	closed stirrups	42.5	56.3
PS2.5	12	0.33	interior	120x120x6	20	5090	9.8x9.8x72	plate stirrups	65.5	73.1
PS3.5	12	0.33	interior	120x120x6	20	5090	9.8x9.8x72	plate stirrups	65.5	73.1
HS2.5	12	0.33	interior	120x120x6	20	5090	9.8x9.8x72	headed studs	65.5	N/A

Specimen ID	Maximum drift, %	Code
2CS	8	ACI-318-99
3SL	8	ACI-318-99
4HS	8	ACI-318-99
MG-5	7.3	ACI-318-95
6CS	5.3	ACI-318-71
7CS	6	ACI-318-71
8CS	5.75	ACI-318-71
PS2.5	10	ACI-318-05
PS3.5	4	ACI-318-05
HS2.5	7	ACI-318-05

Table A5: Reinforced concrete specimens with shear reinforcement, $0.4 \leq \text{GSR} < 0.6$

Specimen ID	Authors (Referred to the references)	GSR	Test configuration	Slab size (in x in x in)	Span to depth ratio	fc' as tested (psi)	Column size (in)	Shear reinforcement type	Flexural reinf. actual f_y (ksi)	Shear reinf. actual f_y (ksi)
A4-S	14	0.4	interior	112x112x4.5	25	4480	W10x88, h=64.3	CFRP stirrups	65.8	116
B4-S	14	0.4	interior	112x112x4.5	25	4480	W10x88, h=64.3	CFRP stirrups	65.8	116
SJB-1	17	0.48	interior	74.8x74.8x5.9	32	4669	9.8x9.8x54.7	headed studs	57.3	66.7
SJB-2	17	0.47	interior	74.8x74.8x5.9	32	4974	9.8x9.8x54.7	headed studs	57.3	66.7
SJB-3	17	0.48	interior	74.8x74.8x5.9	32	4698	9.8x9.8x54.7	headed studs	57.3	66.7
SJB-4	17	0.43	interior	74.8x74.8x5.9	32	5757	9.8x9.8x54.7	headed studs	57.3	66.7
SJB-5	17	0.47	interior	74.8x74.8x5.9	32	4843	9.8x9.8x54.7	headed studs	57.3	66.7
SJB-8	17	0.46	interior	74.8x74.8x5.9	32	5075	9.8x9.8x54.7	headed studs	57.3	66.7
SJB-9	17	0.49	interior	74.8x74.8x5.9	32	4524	9.8x9.8x54.7	headed studs	57.3	66.7
17c	19	0.54	interior	228x228x7.1	32	5340	12x12x78.8	stirrups	81.6 & 78 & 80	87
18c	19	0.44	interior	228x228x7.1	32	5020	12x12x78.8	headed studs	81.6 & 78	72.5
18d	19	0.44	interior	228x228x7.1	32	5020	12x12x78.8	headed studs	81.6 & 78	72.5

Specimen ID	Maximum drift, %	Code
A4-S	8	ACI-318-63
B4-S	8.2	ACI-318-63
SJB-1	5.8	A23.3 & MC-90
SJB-2	5.8	A23.3 & MC-90
SJB-3	5.8	A23.3 & MC-90
SJB-4	7.5	A23.3 & MC-90
SJB-5	7.5	A23.3 & MC-90
SJB-8	5.8	A23.3 & MC-90
SJB-9	7.5	A23.3 & MC-90
17c	5	ACI-318-05
18c	4	ACI-318-05
18d	4	ACI-318-05
17d	5	ACI-318-05

Table A6: Post-tensioned specimens with shear reinforcement, $0.2 \leq \text{GSR} < 0.4$

Specimen ID	Authors (Referred to the references)	GSR	Test configuration	Slab size (in x in x in)	Span to depth ratio	fc' as tested (psi)	Column size (in)	Strand type	Strand f _y (ksi)	Flexural reinf. actual f _y (ksi)
S5 (I)	20	0.33	interior	156x84x5.5	28.3	3600	14x14x101.5	Φ12.7 mm seven-wire strands	191	66 & 66.6
C2 (C)	21	0.27	corner	144x144x3.625	39.7	6130	7.7x7.7x51.5	Φ9.5 mm strands	270	68
PI-B50	22	0.39	interior	181x142x5.1	36	4684	11.8x11.8x82	Φ12.7 mm seven-wire strands	270	51
PI-B30	22	0.24	interior	181x142x5.1	36	4684	11.8x11.8x82	Φ12.7 mm seven-wire strands	270	51
PI-D50	22	0.39	interior	181x142x5.1	36	4684	11.8x11.8x82	Φ12.7 mm seven-wire strands	270	51
PI-D30	22	0.24	interior	181x142x5.1	36	4684	11.8x11.8x82	Φ12.7 mm seven-wire strands	270	51
PE-B50	7	0.34	exterior	94.5x141.7x5.1	18.5	4684	11.8x11.8x82	Φ12.7 mm seven-wire strands	270	67.5
PI-B50X	26	0.38	interior	181x142x5.1	36	4684	11.8x11.8x82	Φ12.7 mm seven-wire strands	225	67.5
PI-D50X	26	0.38	interior	181x142x5.1	36	4684	11.8x11.8x82	Φ12.7 mm seven-wire strands	225	67.5

Specimen ID	fpc (psi)	Maximum drift, %	Code	Comments
S5 (I)		2.25	ACI-318-77	
C2 (C)	193	3.5	ACI-318-89	
PI-B50	175.5	3.3	ACI-318-05 & IBC-03	
PI-B30	175.5	5.9	ACI-318-05 & IBC-03	
PI-D50	175.5	4.2	ACI-318-05 & IBC-03	
PI-D30	175.5	6	ACI-318-05 & IBC-03	
PE-B50	174	4.3	ACI-318-05	
PI-B50X	175	2.1	ACI-318-05	Slab bottom reinforcement through the column was not provided
PI-D50X	175	2.8	ACI-318-05	Slab bottom reinforcement through the column was not provided

Table A7: Post-tensioned specimens with shear reinforcement, $0.4 \leq \text{GSR} < 0.6$

Specimen ID	Authors (Referred to the references)	GS R	Test configuration	Slab size (in x in x in)	Span to depth ratio	fc' as tested (psi)	Column size (in)	Strand type	Strand f _y (ksi)	Flexural reinf. actual f _y (ksi)
S1	23	0.53	edge	236x236x5.9	40	5191	9.8x9.8x42.5	Φ13mm seven-wire strands	241.7	54.4
S2 (E)	20	0.44	exterior	85x84x5.5	15.5	4200	14x14x101.5	Φ12.7mm seven-wire strands	191	66 & 66.6
no ID	25	0.46	interior	224.4x224.4x4.7	47.5	5858	19.7x9.8x71.7x7.7x51.5	Φ12.7mm seven-wire strands	270	73
C1 (C)	21	0.4	corner	144x144x3.625	39.7	5890	7.9x7.9x52.5	Φ9.5 mm strands	270	68
I3 (I)	24	0.55	interior	147x147x3.5	42	4010	11.8x11.8x8.2	Φ12.7mm seven-wire strands	270	78.4
PI-B70	26	0.53	interior	181x142x5.1	36	4684	11.8x11.8x8.2	Φ12.7mm seven-wire strands	225	67.5
PI-B70X	26	0.53	interior	181x142x5.1	36	4684	11.8x11.8x8.2	Φ12.7mm seven-wire strands	225	67.5

Specimen ID	fpc (psi)	Maximum drift, %	Code	Comments
S1	121	4.58	ACI-318-83	designed to be similar to a certain range of buildings in Thailand
S2 (E)		1.9	ACI-318-77	
no ID	168	2	N/A	
C1 (C)	193	3.8	ACI-318-89	
I3 (I)	205	2.26	ACI-318-89	
PI-B70	175	2.8	ACI-318-05	
PI-B70X	175	0.8	ACI-318-05	Slab bottom reinforcement through the column was not provided

All of the tests were stopped before reaching full collapse of the specimens.

B. Types of Loading

i. Reversed cyclic

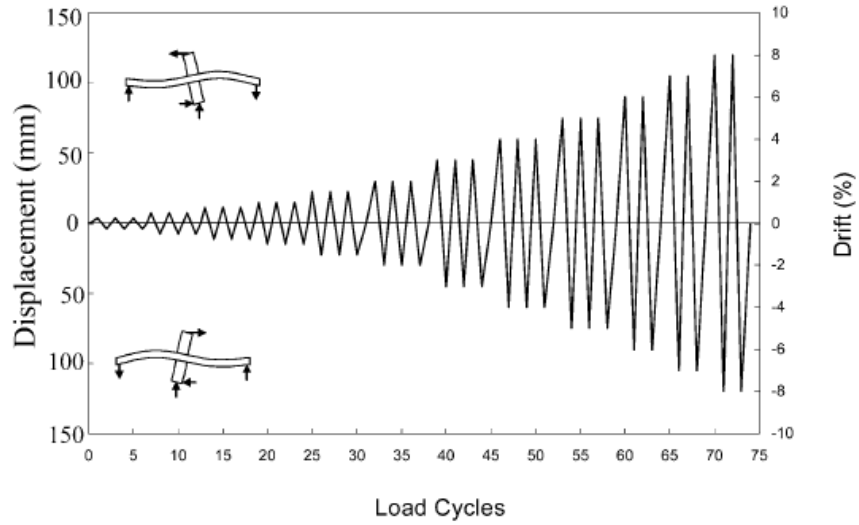


Figure B1: Illustrative uniaxial cyclic loading history of an interior specimen,
Stark, Binici and Bayrak, 2005

Table B1: Illustrative uniaxial cyclic load history of an interior specimen,
Stark, Binici and Bayrak, 2005

Load Step #	Drift, %	Number of cycles, n
1	± 0.25	3
2	± 0.50	3
3	± 0.75	3
4	± 1.0	3
5	± 1.5	3
6	± 2.0	3
7	± 3.0	3
8	± 4.0	3
9	± 5.0	3
10	± 6.0	2
11	± 7.0	2
12	± 8.0	2

ii. Repeated

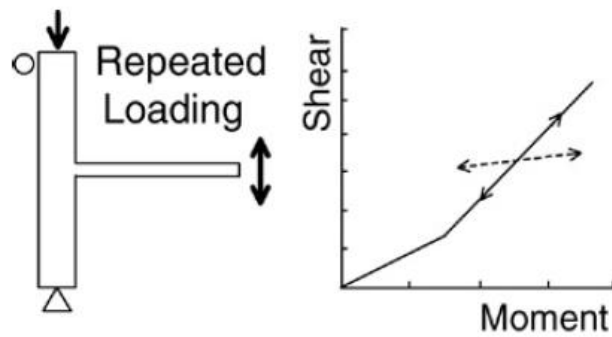


Figure B2: Illustrative repeated loading configuration on an exterior specimen, Trongtham and Hawkins, 1977

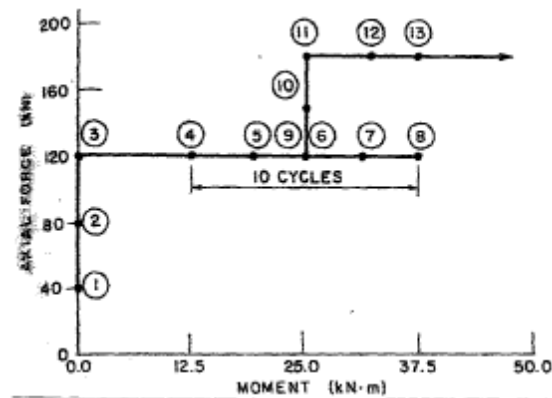


Figure B3: Illustrative repeated loading history, Dilger and Shatila, 1989

C. Test Frame Configurations

i. Interior

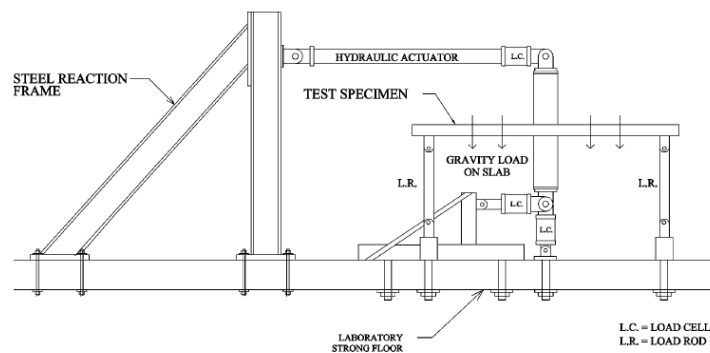


Figure C1: Illustrative test configuration of an interior specimen, Robertson and Johnson, 2006

ii. Exterior

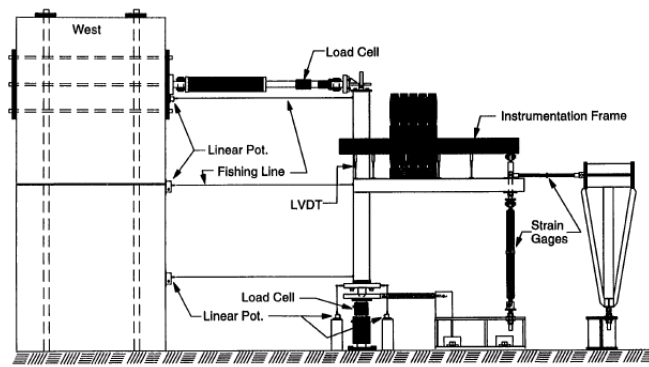


Figure C2: Illustrative test configuration of an exterior specimen, Martinez-Cruzado, 1993

D. Backbone Curves

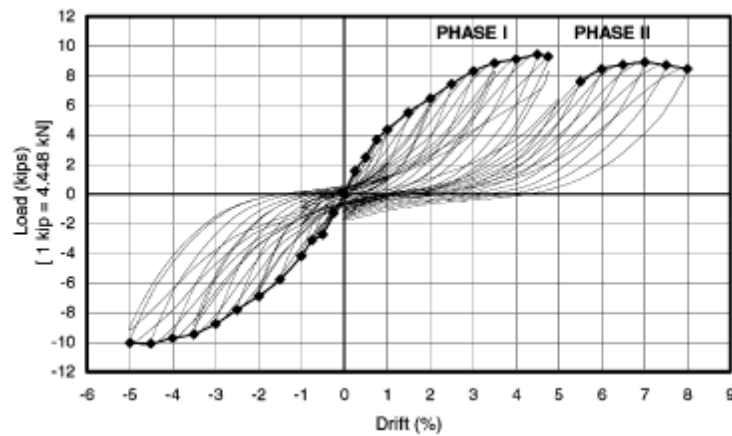


Figure D1: Hysteretic response and backbone curve for specimen 2CS

Robertson, Kawai, Lee and Enomoto, 2002

E. Collected data for yielding and punching states

Table E1: Reinforced concrete specimens with shear reinforcement

(a) $0.2 < V_g/V_0 < 0.4$

Specimen ID	Reference number	yielding		punching	
		demand	f	demand	f
2CS	6	2.56	1	8.0	0
3SL	6	2.13	1	8.0	0
4HS	6	2.38	1	8.0	0
MG-5	15	0.89	1	6.5	1
6CS	18	2.12	1	8.3	1
7CS	18	1.6	1	8.2	1
8CS	18	2.3	1	8.8	1
PS2.5	12	2.2	1	4.85	1
PS3.5	12	1.38	1	3.5	1
HS2.5	12	1.23	1	5	1
X_m		1.79		4.76	
β		0.35		0.46	

(b) $0.4 \leq V_g/V_0 < 0.6$

Specimen ID	Reference number	yielding		punching	
		demand	f	demand	f
A4-S	14	1.69	1	8.3	0
B4-S	14	1.38	1	8.3	0
SJB-1	17	1.29	1	4.58	1
SJB-2	17	2.16	1	4.9	1
SJB-3	17	1.54	1	5.2	1
SJB-4	17	1.89	1	7.3	1
SJB-5	17	1.95	1	7.43	1
SJB-8	17	1.7	1	5.6	1
SJB-9	17	1.95	1	7.42	1
17c	19	1.33	1	2.5	1
18c	19	1.2	1	2.5	1
18d	19	1	1	2	1
X_m		1.55		3.05	
β		0.23		0.5	

Table E2: Post-tensioned specimens without shear reinforcement

(a) $0.2 < V_g/V_0 < 0.4$

Specimen ID	Reference number	yielding		punching	
		demand	f	demand	f
S5 (I)	20	1.1	1	2.25	1
C2 (C)	21	0.46	1	3.33	1
PI-B50	22	1.85	1	3.3	1
PI-B30	22	1.79	1	5.9	1
PI-D50	22	1.125	1	4	1
PI-D30	22	1	1	5.4	1
PE-B50	7	0.77	1	3.3	1
PI-B50X	26	1	1	1.75	1
PI-D50X	26	1.2	1	2.75	1
X_m		0.99		3.1	
β		0.39		0.34	

(b) $0.4 < V_g/V_0 < 0.6$

Specimen ID	Reference number	yielding		punching	
		demand	f	demand	f
S1	23	0.6	1	4.58	1
S2 (E)	20	0.35	1	1.9	1
no ID	25	0.8	1	2	1
C1 (C)	21	0.75	1	3.5	1
I3 (I)	24	1	1	1.6	1
PI-B70	26	1.5	1	2.75	1
PI-B70X	26	0.44	1	0.75	1
X_m		0.62		1.88	
B		0.39		0.53	

